

# Radiation damage evaluation on concrete shielding for nuclear physics experiments

B. Pomaro · V. A. Salomoni · F. Gramegna ·  
G. Prete · C. E. Majorana

Received: 4 August 2010 / Accepted: 11 October 2011 / Published online: 3 November 2011  
© Springer-Verlag 2011

**Abstract** Concrete is commonly used as a biological shield against nuclear radiation. As long as, in the design of nuclear facility, its load carrying capacity is required together with its shielding properties, changes in the mechanical properties due to nuclear radiation are of particular significance and may have to be taken into account in such circumstances. The study presented here allows for reaching first evidences on the behavior of concrete when exposed to nuclear radiation in order to evaluate the consequent effect on the mechanical field, by means of a proper definition of the radiation damage, strictly connected with the strength properties of the building material. Experimental evidences on the decay of the elastic modulus of concrete have allowed for implementing the required damage law within a 3D F.E. research code which accounts for the coupling among moisture, heat transfer and the mechanical field in concrete treated as a fully coupled porous medium. The upgrade of the numerical model allows for assessing the durability of concrete under

the effects of a radioactive environment; considerations on the ultimate strength resource in the lifetime of a nuclear structure can finally lead to its restoration in the damaged parts of the concrete slabs to preserve their load bearing capacity. The development of the damage front in a concrete shielding wall is analyzed under neutron radiation and results within the wall thickness are reported for long-term radiation spans and several concrete mixtures in order to discuss the resulting shielding properties.

**Keywords** Shielding · Radioactive ion beams · Damage · Concrete durability

## 1 Introduction

Irradiation in the form of either fast and thermal neutrons, primary gamma rays or gamma rays produced as a result of neutron capture can affect concrete. Changes in the properties of concrete appear to depend primarily on the behavior of concrete aggregates that can undergo a volume change when exposed to radiation. Radiation damage in concrete aggregates is caused by changes in the lattice structure of the minerals in the aggregates. Fast neutrons are mainly responsible for the considerable growth, caused by atomic displacements, that has been measured in certain aggregates (e.g. flint). Quartz aggregates, made of crystals with covalent bonding, seem to be more affected by radiation than calcareous aggregates that contain a weaker ionic bonding. Neutron fluences of the order of  $1 \times 10^{19}$  n/cm<sup>2</sup> and gamma radiation doses of  $10^{10}$  rad seem to become critical for concrete strength.

Particularly, the study has been motivated by an ongoing research program in conjunction with the National Laboratories of Legnaro (Padua, Italy) within the SPES Project

---

B. Pomaro · V. A. Salomoni (✉) · C. E. Majorana  
Department of Structural and Transportation Engineering,  
University of Padua, Via F. Marzolo, 9, 35131 Padua, Italy  
e-mail: salomoni@dic.unipd.it

B. Pomaro  
e-mail: pomaro@dic.unipd.it

C. E. Majorana  
e-mail: majorana@dic.unipd.it

F. Gramegna · G. Prete  
INFN, National Institute of Nuclear Physics,  
National Laboratories of Legnaro (Pd),  
Viale dell'Università, 2, 35020 Legnaro (Pd), Italy  
e-mail: fabiana.gramegna@lnl.infn.it

G. Prete  
e-mail: gianfranco.prete@lnl.infn.it

(SPES Executive Summary 2008 [17]) and it represents a first step towards the assessment of radiation damage induced by nuclear radiation in concrete vessels; the facility to be built will be directed to the production of special radioactive heavy ion beams from a primary proton beam impinging on a target made of fissionable material, where fission reactions are expected to take place, thus representing ideally a point-source of neutrons in the specific problem.

The phenomenon has been treated with a macroscopic approach under the assumptions made in Sect. 2.2 for the radiation field.

An already available F.E. code able to perform fully coupled hygro-thermo-mechanical analyses for cementitious materials has been upgraded to take into account the effects of nuclear radiation on the material via the introduction of a new damage variable; specifically, radiation damage is defined based on experimental evidences and it is supposed acting in conjunction with the already implemented chemo-thermo-mechanical damage; numerical results which lead to quantify the decay in stiffness and the full hygro-thermo-mechanical response of a concrete wall under neutron radiation exposure are reported and discussed.

## 2 The mathematical model

The F.E. model adopted to perform radiation-induced damage analyses is the 3D research code NEWCON3D [1, 10, 19, 23–31, 34, 36–40]. Concrete is treated as a multiphase system where the micropores of the skeleton are partially filled with liquid water, both in the form of bound or absorbed water and free or capillary water, and partially filled with a gas mixture composed of dry air (non-condensable constituent) and water vapour (condensable), supposed to behave like an ideal gas [1, 24, 27, 40].

When higher than standard temperatures are taken into account several phenomena are considered within the model, dealing with concrete as a porous medium: heat conduction, vapour diffusion and liquid water flow in the voids.

As regards the mechanical field, the model couples shrinkage, creep, damage and plasticity effects within the constitutive law of the material, here developed starting from a thermodynamic approach.

### 2.1 Thermodynamic formulation

In order to define the thermodynamic framework for a multiphase medium system, accounting for damage, plasticity, autogenous effects and creep, as concrete is modeled

into NEWCON3D, we consider a solid body  $\Omega$  occupying a material volume  $V$  bounded by a surface  $\Sigma$ , whose outer normal is  $\mathbf{n}$ . Let the solid, of mass density  $\rho$ , absorb vapor through its boundary and let  $m$  denote the vapor/fluid mass per unit volume of the solid (i.e. moisture concentration). Also, let  $\mathbf{x}$  be the position of a solid mass particle in the deformed configuration that corresponds to the place  $\mathbf{X}$  in the undeformed state, and let  $\mathbf{f}$  and  $\mathbf{q}$  denote fluxes of mass vapor and heat, respectively, and  $\mathbf{v}$  the velocity of the solid particles.

In addition, let  $e$  and  $s$  be the internal energy and entropy densities of the solid/vapor mixture per unit solid mass, and let  $\sigma_{ij}$  and  $T$  denote the components of the Cauchy stress due to mechanically applied loads and temperature, respectively.

We consider the solid/fluid mixture as an open system, with the fluid phase at pressure  $\bar{p}$  and density  $\bar{\rho}$ ; we define with  $\bar{e}$  and  $\bar{s}$  the internal energy and entropy densities of the fluid phase, respectively.

Conservation of the solid and fluid masses gives (the dot denotes total derivative with respect to time,  $\Delta$  denotes divergence)

$$\dot{\rho} + \rho \Delta \mathbf{v} = 0 \quad (1)$$

$$\dot{m} = -\Delta \mathbf{f} \quad (2)$$

Conservation of energy over the volume  $\Omega$  is given by the first principle of thermodynamics

$$\frac{d(E + K)}{dt} = P_{(e)} + Q + F \quad (3)$$

where  $E$  and  $K$  are the internal energy and the kinetic energy of the domain  $\Omega$ ,  $P_{(e)}$  is the mechanical power due to external forces,  $Q$  is the heat power received by  $\Omega$ ,  $F$  is the power due to the fluid flow.

If we denote by  $\mathbf{t}$  the volumetric force density and by  $\mathbf{T}$  the surface force density, then  $P_{(e)}$  is given by the Cauchy axiom (repeated indices imply summation, according to tensorial algebra formalism)

$$P_{(e)} = \int_V \mathbf{t}_i v_i dV + \int_\Sigma T_i v_i dA \quad (4)$$

On the other hand,  $Q$  consists in two components: the heat generated in  $\Omega$  due to actions external to  $\Omega$ , defined as  $r$  in the following, and the heat received for conduction through the surface  $\Sigma$

$$Q = \int_V r dV - \int_\Sigma q_i n_i dA \quad (5)$$

$F$  is given by two contributions: the mechanical power due to the vapor flux (notice that  $\mathbf{f}/\bar{\rho}$  is the velocity of the fluid phase) and the rate of internal energy due to the fluid flux [44]

$$F = - \int_{\Sigma} \bar{p} \frac{f_i}{\bar{\rho}} n_i dA - \int_{\Sigma} \bar{e} f_i n_i dA \tag{6}$$

Reminding that [22]

$$P_{(i)} + P_{(e)} = \frac{dK}{dt} \tag{7}$$

the extended formulation of the conservation law that gives the first principle becomes

$$\begin{aligned} \frac{d}{dt} \int_V \rho e dV &= \int_V \sigma_{ij} D_{ij} dV + \int_V r dV - \int_{\Sigma} q_i n_i dA \\ &\quad - \int_{\Sigma} \bar{p} \frac{f_i}{\bar{\rho}} n_i dA - \int_{\Sigma} \bar{e} f_i n_i dA \end{aligned} \tag{8}$$

where

$$P_{(i)} = - \int_V \sigma_{ij} D_{ij} dV \tag{9}$$

$D_{ij}$  being the strain rate tensor

$$D_{ij} = \frac{1}{2} (v_{i,j} + v_{j,i}) \tag{10}$$

which is linked with the strain tensor  $\epsilon$ , in the hypothesis of infinitesimal strain theory, by

$$D = \dot{\epsilon} \tag{11}$$

or, being  $\mathbf{u}$  the displacements vector

$$\epsilon_{ij} = \frac{1}{2} (u_{i,j} + u_{j,i}) \quad v_i = \dot{u}_i \tag{12}$$

Equation 8 must hold for any arbitrary domain  $\Omega$  so that, after applying the Green’s theorem and employing (2), the conservation law in the field of small deformations yields

$$\rho \dot{e} = \sigma_{ij} \dot{\epsilon}_{ij} + r - q_{i,i} - \bar{h}_{,i} f_i + \bar{h} \dot{m} \tag{13}$$

where  $\bar{h}$  is the enthalpy of the fluid phase, function of its pressure  $\bar{p}$ , its mass density  $\bar{\rho}$  and its internal energy density  $\bar{e}$

$$\bar{h} = \frac{\bar{p}}{\bar{\rho}} + \bar{e} \tag{14}$$

The Clausius–Duhem inequality, or second principle, requires

$$\begin{aligned} \frac{d}{dt} \int_V \rho s dV &\geq \int_V \frac{r}{T} dV - \int_{\Sigma} \frac{q_i}{T} n_i dA - \int_{\Sigma} \bar{s} f_i n_i dA \\ &\quad - \int_{\Sigma} \frac{\gamma_i}{T} n_i dA \end{aligned} \tag{15}$$

where the fourth integral expresses the fluid phase contribution for entropy and the last one, depending on a general

quantity  $\gamma$ , is the overall dissipation due to the processes concrete undergo: damage, plasticity, autogenous effects and viscosity.

Again for arbitrary  $\Omega$ , by applying the Green’s theorem to (15) and employing (2), the thermodynamic inequality states

$$\rho \dot{s} + \left(\frac{q_i}{T}\right)_{,i} + \left(\frac{\gamma_i}{T}\right)_{,i} - \frac{r}{T} + \bar{s}_{,i} f_i - \bar{s} \dot{m} \geq 0 \tag{16}$$

We now derive  $r$  from the first principle (see 13) and multiply by  $T > 0$ ; notice that

$$\left(\frac{q_i}{T}\right)_{,i} = \frac{q_{i,i}}{T} - \frac{q_i}{T^2} T_{,i} \tag{17}$$

so we obtain

$$\begin{aligned} \rho (T \dot{s} - \dot{e}) + \sigma_{ij} \dot{\epsilon}_{ij} - \frac{q_i}{T} T_{,i} + \gamma_{i,i} - \bar{h}_{,i} f_i + \bar{h} \dot{m} \\ + T \bar{s}_{,i} f_i - T \bar{s} \dot{m} \geq 0 \end{aligned} \tag{18}$$

Now if we define the Helmholtz free energy

$$\psi = e - Ts \tag{19}$$

and the chemical potential of fluid phase according to Weitsman [44]

$$\bar{\mu} = \bar{h} - T \bar{s} \tag{20}$$

the second principle of thermodynamics for a multiphase system, accounting for damage, plasticity, autogenous effects and creep, in the hypothesis of infinitesimal strains yields

$$\begin{aligned} -\rho (\dot{\psi} + s \dot{T}) + \sigma_{ij} \dot{\epsilon}_{ij} - \frac{q_i + \gamma_i}{T} T_{,i} + \gamma_{i,i} + \bar{\mu} \dot{m} - f_i \bar{\mu}_{,i} \\ - T_{,i} \bar{s}_{,i} f_i \geq 0 \end{aligned} \tag{21}$$

It is to be underlined that the formulation we have here, for a multiphase system able to undergo autogenous effects, elasto-plasticity, damage and creep, turns out to the classical expression of the Clausius–Duhem inequality

$$-\rho (\dot{\psi} + s \dot{T}) + \sigma_{ij} \dot{\epsilon}_{ij} - \frac{q_i}{T} T_{,i} \geq 0 \tag{22}$$

where some terms are generated in addition, due to the newly introduced sources of dissipation, which is in agreement with the approach suggested in [18].

### 2.1.1 Local state approach

With the two main results of thermodynamics being reached, we use now the local state approach to formulate the constitutive equations for concrete as an elastic–plastic material, with damage, autogenous and viscous effects included as well, in the assumptions of infinitesimal deformations and coupling between thermal, hygral and mechanical fields.

Within the local state approach the thermodynamics of a solid continuum, at a point and a given instant of time, is defined as long as the value of a certain number of state variables is known, depending on the space coordinates only and not time-varying [22]. This assumption implies that the evolution of the thermodynamic state can be considered as a sequence of equilibrium states. We distinguish between observable variables and internal variables.

The physical phenomenon here analyzed, i.e. the considered constitutive law for the material under thermo-hygro-mechanical loads, defines itself the first group of variables:  $\boldsymbol{\varepsilon}$  the total strain tensor,  $T$  temperature and  $m$  the moisture mass per unit volume of the solid (moisture concentration), for which the conservation law (2) holds; these quantities are, in fact, strictly necessary to describe the reversible part of the process. The other variables are required when dissipative phenomena occur and, as a consequence, the present state depends also from the history of the problem, which is described by the value in a specific instant of time by the internal variables.

For the plastic free energy, the necessary internal variables are the following: the cumulative plastic strain  $p$ , defined as [22]

$$p = \int_0^t \left[ \frac{2}{3} \dot{\boldsymbol{\varepsilon}}^p(\tau) : \dot{\boldsymbol{\varepsilon}}^p(\tau) \right]^{1/2} d\tau \quad (23)$$

(the symbol  $:$  denoting tensor contraction);  $p$  is a scalar measure of the plastic deformation and, as an always increasing quantity, it is associated to a specific instant in a monotone loading history, and it is not sufficient, alone, to describe more complicated cycling loads, for which one or more kinematic tensor variables are needed. Here we refer to just one hardening variable  $\boldsymbol{\alpha}$ , often coinciding with the plastic deformation ( $\boldsymbol{\alpha} = \boldsymbol{\varepsilon}^p$ ) as in the Prager model for plasticity (linear kinematic hardening).

For the elasto-damaged component of the total free energy, the necessary internal variable is represented by a scalar variable taking into account damage effects due to irreversible changes on the internal structure  $D$ , and a scalar variable  $\beta$  providing the current state of damage -introduced to prescribe the effects of current damage state on the further development of damage, in agreement with [12] in which thermodynamics for elastic–plastic materials with damage is investigated.

For the other two components we assume that the amount of total strain accounting for autogenous effects  $\boldsymbol{\varepsilon}^a$  and the one accounting for relaxation (creep) effects  $\boldsymbol{\varepsilon}^c$  are themselves the internal variables for the two phenomena, in analogy to plasticity, though this approach does not prevent the generality of this topic.

The physical process is named to be thermodynamically admissible if it satisfies the Clausius–Duhem

inequality at each instant of the evolution in time of the process.

The state variables being identified, the Helmholtz free energy of the material per unit volume  $\psi$  needs to be defined. We remind that, in the assumption of infinitesimal strains, the total strain tensor  $\boldsymbol{\varepsilon}$  can be split into the components given by the elastic strain, supposed to be affected by damage  $\boldsymbol{\varepsilon}^{ed}$ , the plastic strain  $\boldsymbol{\varepsilon}^p$ , the autogenous strain  $\boldsymbol{\varepsilon}^a$  and the viscous strain  $\boldsymbol{\varepsilon}^c$ . Under this hypothesis  $\psi$  can be expressed as a superposition of effects: the fraction coming from the elastic behavior, affected by damage  $\psi_e(\boldsymbol{\varepsilon}^{ed}, D, m, T)$ , the one due to the development of microscopic defects  $\psi_d(\beta)$ , the one given by plastic deformation, i.e. hardening process  $\psi_p(p, \boldsymbol{\alpha}, m, T)$ , the one due to autogenous effects (e.g. given by chemical reactions due to carbonation or to the action of chlorides or sulfates)  $\psi_a(\boldsymbol{\varepsilon}^a, m, T)$ , the one linked to relaxation effects, i.e. creep (at low to medium temperatures), which is supposed to evolve into load-induced thermal effects (at high temperatures)  $\psi_c(\boldsymbol{\varepsilon}^c, m, T)$

$$\rho\psi = \rho\psi_e(\boldsymbol{\varepsilon}^e, D, m, T) + \rho\psi_d(\beta) + \rho\psi_p(p, \boldsymbol{\alpha}, m, T) + \rho\psi_a(\boldsymbol{\varepsilon}^a, m, T) + \rho\psi_c(\boldsymbol{\varepsilon}^c, m, T) \quad (24)$$

It has to be noticed that the internal structural changes due to damage are supposed to influence the elastic deformation only, under the assumption that the free energy due to plastic, autogenous and viscous deformation is small in comparison with the elastic one, so that the effects of damage on plasticity, autogenous fields and viscosity can be neglected.

**2.1.1.1 The elastic free energy** As regards the free energy in the elastic field  $\psi_e$ , where damage is supposed to occur, the requirement of its convexity with respect to all the state variables (in order to verify a priori the second law inequality) leads to an expression for  $\psi_e$  -in presence of damage- still quadratic in  $\boldsymbol{\varepsilon}^e$  and  $T$ , as when damage is not accounted for [22]. Generalizing the thermo-elastic approach provided by Lemaitre and Chaboche [22] to coupled thermo-hygro-mechanics, the following expression for the elastic contribution to the total free energy is obtained:

$$\rho\psi_e = \frac{1}{2} (1 - D) \mathbf{D}_T : (\boldsymbol{\varepsilon}^e - \mathbf{k} dT - \boldsymbol{\mu} dm) : (\boldsymbol{\varepsilon}^e - \mathbf{k} dT - \boldsymbol{\mu} dm) + C dT^2 + M dm^2 \quad (25)$$

in which  $\boldsymbol{\varepsilon}^e$  is the elastic strain tensor of the undamaged material,  $\mathbf{D}_T$  the tangent stiffness tensor,  $\mathbf{k}$  the tensor containing thermal expansion coefficients,  $\boldsymbol{\mu}$  the tensor containing the coefficients of hygrometric expansion, so that  $\mathbf{k}dT$  and  $\boldsymbol{\mu}dm$  represent the thermal and hygral dilation, respectively.

We derive here the state laws starting from the employed potential: the specific free energy  $\psi$ . Thanks to the decomposition of the total strain tensor into

$$\varepsilon = \varepsilon^e + \varepsilon^p + \varepsilon^a + \varepsilon^c \tag{26}$$

the potential expressed in Eq. 24 can be written, in general, as dependent on the following quantities

$$\psi = \psi([\varepsilon - \varepsilon^p - \varepsilon^a - \varepsilon^c], m, T, V_k) = \psi(\varepsilon^e, m, T, V_k) \tag{27}$$

where we denote by  $V_k$  the internal variables defined in Sect. 2.1.1.

For the derivative of  $\psi$ , then

$$\frac{\partial \psi}{\partial \varepsilon^e} = \frac{\partial \psi}{\partial \varepsilon} = -\frac{\partial \psi}{\partial \varepsilon^p} = -\frac{\partial \psi}{\partial \varepsilon^a} = -\frac{\partial \psi}{\partial \varepsilon^c} \tag{28}$$

By differentiating  $\psi$  with respect to time

$$\dot{\psi} = \frac{\partial \psi}{\partial \varepsilon^e} : \dot{\varepsilon}^e + \frac{\partial \psi}{\partial m} \dot{m} + \frac{\partial \psi}{\partial T} \dot{T} + \frac{\partial \psi}{\partial V_k} \dot{V}_k \tag{29}$$

and substituting within the second principle, Eq. 21 in tensorial notation yields ( $\nabla$  denotes the gradient and  $\Delta$ , again, the divergence)

$$\begin{aligned} \left( \boldsymbol{\sigma} - \rho \frac{\partial \psi}{\partial \varepsilon^e} \right) : \dot{\varepsilon}^e + \boldsymbol{\sigma} : \dot{\varepsilon}^p + \boldsymbol{\sigma} : \dot{\varepsilon}^a + \boldsymbol{\sigma} : \dot{\varepsilon}^c \\ - \rho \left( s + \frac{\partial \psi}{\partial T} \right) \dot{T} - \rho \frac{\partial \psi}{\partial V_k} \dot{V}_k \pm \frac{\mathbf{q} + \boldsymbol{\gamma}}{T} \cdot \nabla T + \Delta \boldsymbol{\gamma} \\ + \left( \bar{\mu} - \rho \frac{\partial \psi}{\partial m} \right) \dot{m} - \mathbf{f} \cdot \nabla \bar{\mu} - \nabla T \cdot \nabla \bar{s} \cdot \mathbf{f} \geq 0 \end{aligned} \tag{30}$$

We make use of the classical hypothesis of thermo-elasticity to reset some terms to zero at the same time. In addition, if also the terms  $\Delta \boldsymbol{\gamma}$ , and  $\mathbf{f} \cdot \nabla \bar{\mu}$  tend to zero, the inequality holding for any  $\dot{\varepsilon}^e$ ,  $\dot{m}$ ,  $\dot{T}$ , gives the state laws in thermo-elasticity for the observable variables

$$\begin{aligned} \boldsymbol{\sigma} = \rho \frac{\partial \psi}{\partial \varepsilon^e} = (1 - D) \mathbf{D}_T : (\varepsilon^e - \mathbf{k} dT - \boldsymbol{\mu} dm) \\ = \bar{\mathbf{D}}_T : (\varepsilon^e - \mathbf{k} dT - \boldsymbol{\mu} dm) \end{aligned} \tag{31}$$

and

$$s = -\frac{\partial \psi}{\partial T} \quad \bar{\mu} = \rho \frac{\partial \psi}{\partial m} \tag{32}$$

Equation 31 shows that the free energy is a stress potential or, in other words, that the stress tensor  $\boldsymbol{\sigma}$  is the conjugate thermodynamic variable for the elastic strain tensor. Moreover, according to (31), the stress tensor  $\boldsymbol{\sigma}$  can be considered as a modified stress tensor  $\bar{\boldsymbol{\sigma}}$  in presence of damage [22]

$$\bar{\boldsymbol{\sigma}} = \frac{\boldsymbol{\sigma}}{1 - D} = \mathbf{D}_T : (\varepsilon^e - \mathbf{k} dT - \boldsymbol{\mu} dm) \tag{33}$$

Equations 32, on the other hand, defines the specific entropy and the chemical potential as the conjugate variables to temperature and moisture concentration, respectively.

*2.1.1.2 The free energy due to creep* Acknowledged analytic expressions for the introduced free energy components are available in literature for  $\psi_e$  and  $\psi_c$ . Focusing on the component of the total free energy due to viscous effects  $\psi_c$ , its definition implies to analyze the class of thermodynamically admissible creep and relaxation functions,  $\mathbf{c}$  and  $\mathbf{r}$  respectively, in the classic visco-elastic constitutive equations, relating the deformation and stress tensor  $\boldsymbol{\varepsilon}$  and  $\boldsymbol{\sigma}$

$$\boldsymbol{\varepsilon} = \mathbf{c} \circ \boldsymbol{\sigma} \quad \boldsymbol{\sigma} = \mathbf{r} \circ \boldsymbol{\varepsilon} \tag{34}$$

where the operator  $\circ$  is the Stieltjès convolution. It is in fact shown that the field of thermodynamically admissible creep-relaxation functions is larger than the traditional set of monotone positive definite functions used in practice (exponential or power functions) and includes several non-monotone and even locally negative functions [13, 14]. Particularly, the use of exponentials is prior to power functions due mainly to historical reasons, i.e. linear viscosity was born in connection with the study of polymers' behavior and, only later on, with creep on porous materials, where the power integral kernels  $K$ , required by the heredity theory were introduced in the Volterra integral form of the constitutive law (one-dimensional domain)

$$\sigma(t) = \int_{-\infty}^t K(0, t - v) d\varepsilon(v) \quad K(0, t) = r(t) \tag{35}$$

in which  $r(t)$  is the relaxation function and the integral is Stieltjes integral.

One of the expressions for the density of the Helmholtz free energy, still most frequently applied, comes from Staverman-Schwarzl [42, 43], established for exponential relaxation functions for polymers in isothermal conditions

$$\psi_c(t) = \frac{1}{2} \int_0^t \int_0^t r(2t - u - v) d\varepsilon(v) d\varepsilon(u) \tag{36}$$

where the lower limits of the integrals are justified when loading starts at time  $t = 0$  with a jump; Eq. 36 represents a particular case of the more general expression

$$\psi_c(t) = \frac{1}{2} \int_{-\infty}^t \int_{-\infty}^t K(t - u, t - v) d\varepsilon(v) d\varepsilon(u) \tag{37}$$

where  $K$  is such a kernel that functional  $\psi_c$  in Eq. 37 is non-negative definite.

It is in fact to be noticed that (36) comes from (37) when the following holds

$$K(x, y) = K(x + y) \tag{38}$$

and in (36)  $r(t)$  is a function of the relaxation spectrum  $\rho(\mu)$

$$r(t) = \int_0^\infty \rho(\mu)e^{-\frac{t}{\mu}}d\mu + r_\infty \tag{39}$$

$r_\infty$  being the long-term modulus.

Non isothermal conditions were successively taken into account by Staverman assuming small changes of temperature, leading to a similar expression, though in incremental form [43].

As shown by Eq. 36, the Staverman-Schwarzl’s expression is a non-aging-like model for visco-elastic materials, since only heredity is taken into account i.e. the relaxation function, within the Volterra integral, is dependent just on the time lag  $t-u-v$  (duration of unit constant stress), and not separately on  $t, u, v$ . This second scenario would account for the description of the typical time-hardening process exhibited by concrete under solidification, mainly due to the mass growth of cement hydration products per unit volume.

A thermodynamic formulation for ageing visco-elasticity has been more recently suggested by Bazant and Huet [2], by generalization of the Staverman-Schwarzl’s formula; after considerations on the integration domain, an expression for  $\psi_c$  is given that involves double Stieltjes integration, over a square domain for the strain history, of a quadratic expression depending only on a symmetrized form of the relaxation function, according to the following

$$\psi_c(t) = \frac{1}{2} \int_0^t \int_0^t f(t, u, v)d\varepsilon(v)d\varepsilon(u) \tag{40}$$

where  $f(t, u, v)$  is found to be symmetric with respect to  $u$  and  $v$

$$f(t, u, v) = f(t, v, u) \tag{41}$$

and

$$f(t, u, v) = \min[R(2t - v, u), R(2t - u, v)] \tag{42}$$

with  $R(t, t')$  relaxation function for the aging material.

Expression (40) suggested by Bazant and Huet for the free energy is shown to be a potential for stress, in fact after differentiation of (40) one gets

$$\begin{aligned} \frac{\partial \psi_c(t)}{\partial \varepsilon(t)} &= \frac{1}{2} \int_0^t \min[R(2t - u, t), R(2t - t, u)]d\varepsilon(u) \\ &+ \frac{1}{2} \int_0^t \min[R(2t - t, v), R(2t - v, t)]d\varepsilon(v) \end{aligned} \tag{43}$$

if we substitute  $t = u + \Delta$ , with  $\Delta > 0$ , and we suppose the material to harden rather than to soften, as it ages, i.e.

$$R(t + \Delta, t' + \Delta) \geq R(t, t'), \tag{44}$$

then (i) in the first integral of Eq. 43 the second of the two relaxation functions is the minimum and (ii) in the second integral the first relaxation function is the minimum, so that

$$\begin{aligned} \frac{\partial \psi_c(t)}{\partial \varepsilon(t)} &= \frac{1}{2} \int_0^t R(t, u)d\varepsilon(u) + \frac{1}{2} \int_0^t R(t, v)d\varepsilon(v) \\ &= \int_0^t R(t, t')d\varepsilon(t') = \sigma^c(t) \end{aligned} \tag{45}$$

which proves that the free energy per unit volume of the material is a potential for the stress and allows to obtain a constitutive equation for ageing visco-elasticity consistent with continuum thermodynamics. Relationship (45) holds for viscoelastic ageing materials exhibiting instantaneous elasticity, however in absence of instantaneous elasticity it is sufficient to add the (instantaneous) purely viscous stress to the stress obtained from the potential, to have the correct stress, so the main relationship (45) still holds.

*2.1.1.3 The other state laws and the complementary laws* In analogy to what stated for the stress tensor, temperature and moisture concentration in Sect. 2.1.1.1, the conjugate forces corresponding to the internal state variables  $D, p, \alpha, \beta, \varepsilon^a$  and  $\varepsilon^c$ :  $Y, R, \mathbf{A}, B, \sigma^a, \sigma^c$  respectively, can be found by taking into account the different components of the total free energy  $\rho\psi$

$$\begin{aligned} Y &= \rho \frac{\partial \psi_e}{\partial D} = -\frac{1}{2} \mathbf{D}_T : (\varepsilon^e - \mathbf{k} dT - \boldsymbol{\mu} dm) \\ &: (\varepsilon^e - \mathbf{k} dT - \boldsymbol{\mu} dm) R = \rho \frac{\partial \psi_p}{\partial p} \quad \mathbf{A} = \rho \frac{\partial \psi_p}{\partial \boldsymbol{\alpha}} \\ B &= \rho \frac{\partial \psi_d}{\partial \beta} \quad \sigma^a = -\rho \frac{\partial \psi_a}{\partial \varepsilon^a} \quad \sigma^c = -\frac{\partial \psi_c}{\partial \varepsilon^c} \end{aligned} \tag{46}$$

In order to describe the inelastic dissipative process, as well as the evolution of the internal state variables, it is necessary to refer to the dissipation potential, i.e. a function continuous and convex with respect to the flux variables (i.e. time derivatives of the internal state variables and heat flux). By means of such a function the relationships between flux variables and dual variables given by the conjugate forces, i.e. the complementary laws, can be found.

If the expressions of the dissipation potential and its dual potential, function of the conjugate forces, are, respectively

$$\begin{aligned} \varphi &= \varphi\left(\dot{\varepsilon}^e, \dot{D}, \dot{p}, \dot{\boldsymbol{\alpha}}, \dot{\beta}, \varepsilon^a, \varepsilon^c, \frac{\mathbf{q}}{T}, \mathbf{f}\right) \\ \varphi^* &= \varphi^*(\boldsymbol{\sigma}, Y, R, \mathbf{A}, B, \mathbf{l}, \mathbf{i}) \end{aligned} \tag{47}$$

where  $\mathbf{l}$  and  $\mathbf{i}$  are the thermodynamic conjugate forces related to heat flux  $\mathbf{q}$  and moisture flux  $\mathbf{f}$ , respectively



$$\mathbf{l} = \nabla T \quad \mathbf{i} = \nabla \bar{h} \tag{48}$$

then, the complementary laws are the following

$$\begin{aligned} \dot{\varepsilon}^p &= \frac{\partial \varphi^*}{\partial \boldsymbol{\sigma}} \quad \dot{D} = -\frac{\partial \varphi^*}{\partial Y} \quad \dot{p} = -\frac{\partial \varphi^*}{\partial R} \quad \dot{\alpha} = -\frac{\partial \varphi^*}{\partial \mathbf{A}} \\ \dot{\beta} &= -\frac{\partial \varphi^*}{\partial B} \quad \varepsilon^a = \frac{\partial \varphi^*}{\partial \boldsymbol{\sigma}} \quad \varepsilon^c = \frac{\partial \varphi^*}{\partial \boldsymbol{\sigma}} \quad \frac{\mathbf{q}}{T} = -\frac{\partial \varphi^*}{\partial \mathbf{l}} \quad \mathbf{f} = -\frac{\partial \varphi^*}{\partial \mathbf{i}} \end{aligned} \tag{49}$$

It has to be underlined that the first law leads to the plasticity law whereas the following four relationships represent the evolution laws for the internal state variables, particularly the second is the so-called property of normality for the damage variable  $D$ .

Now, if the flux vector  $\mathbf{J}$  is defined as

$$\mathbf{J} = \rho \left\{ \dot{\varepsilon}^p, \dot{D}, \dot{p}, \dot{\alpha}, \dot{\beta}, \varepsilon^a, \varepsilon^c, \mathbf{q}, \mathbf{f} \right\}^T \tag{50}$$

and its thermodynamic conjugate force vector  $\mathbf{X}$  as follows

$$\mathbf{X} = \left\{ \boldsymbol{\sigma}, Y, R, \mathbf{A}, B, \frac{\mathbf{l}}{T}, \mathbf{i} \right\} \tag{51}$$

then the rate of entropy production can be expressed as the product between the two, and the second principle requires it is non-negative

$$\begin{aligned} \mathbf{X} \cdot \mathbf{J} &= \boldsymbol{\sigma} : \dot{\varepsilon}^p - Y\dot{D} - R\dot{p} - \mathbf{A} : \dot{\alpha} - B\dot{\beta} + \boldsymbol{\sigma} : \varepsilon^a + \boldsymbol{\sigma} : \varepsilon^c \\ &\quad - \frac{1}{T} \mathbf{l} \cdot \mathbf{q} - \mathbf{i} \cdot \mathbf{f} \geq 0 \end{aligned} \tag{52}$$

If the uncoupling among intrinsic, thermal and hygral dissipation is conceived (which does not imply the uncoupling of effects) and the hardening effect is supposed to happen without damage and, viceversa, damage occurs without a macroscopic plastic deformation, the following inequalities hold separately

$$\begin{aligned} \boldsymbol{\sigma} : \dot{\varepsilon}^p - R\dot{p} - \mathbf{A} : \dot{\alpha} - B\dot{\beta} + \boldsymbol{\sigma} : \varepsilon^a + \boldsymbol{\sigma} : \varepsilon^c &\geq 0 \\ -Y\dot{D} &\geq 0 \end{aligned} \tag{53}$$

which,  $Y$  being quadratic, definite positive according to Eq. 46, states the increase of damage in time, in order to fulfill the second principle of thermodynamics.

Equation 52 represents another expression for the Clausius–Duhem inequality (21) where the extra entropy flux  $\gamma$  accounted for the dissipative processes -in addition to heat dissipation and fluid flow dissipation- i.e. the mechanical dissipative processes connected with damage, autogenous effects and (irreversible) creep, which appear in (52).

### 2.2 The radiation field

The type of radiation considered consists in neutron radiation, to answer the specificity of the problem represented

by the SPES Project, which will be illustrated in the following.

Particularly, the effects of nuclear radiation on several types of concretes commonly used as shielding materials are here investigated, in order to evaluate for each of them not only their shielding capacity against neutrons as source of radiation, but also the effects on the mechanical response of the material under such an extreme condition.

A macroscopic neutron behavior is considered in the following to describe the attenuation of radiation in matter; in other words two distinct approximate approaches of the more rigorous transport theory are preferred to the deterministic approach given by the solution of the transport equation by Boltzmann as well as to the stochastic approach by Monte Carlo techniques.

Particularly the two approaches are: the diffusion theory, which applies to thermal neutrons, and the two-group theory, which allows for getting the fast group equation in a semi-infinite plane geometry [41]. They both develop from the above mentioned integro-differential equation by Boltzmann, obtained by considering the inflow and outflow balance of particles through the surface of an arbitrary closed volume in a steady state condition for the radiation field. These approaches renounce to solve the problems associated to primary neutrons attenuation, such as the production of photons during inelastic scattering, the capture of thermal neutrons leading to capture gamma photons and even production of secondary neutrons as a result of fission reactions; nevertheless they offer, in their simplified way, acceptable estimates of the expected flux density field [11, 20, 41].

The basic hypothesis of the diffusion theory is that the neutron current  $\mathbf{I}$  is isotropic and is given by

$$\mathbf{I} = -D\nabla\Phi \tag{54}$$

thus leading to an equation of the type

$$-D\nabla^2\Phi + \Sigma_a\Phi - S = 0 \tag{55}$$

where  $\Phi$  is the flux density (for instance in [n/(cm<sup>2</sup> s)]),  $S$  is the source term,  $\Sigma_a$  is the absorption cross-section and  $D$  a diffusion coefficient, defined in a simple diffusion theory by

$$D = \frac{\lambda_s}{3} \tag{56}$$

$\lambda_s$  being the scattering mean free path.

The solution of a plane source in an infinite medium can be derived from this approximated theory by imposing proper boundary conditions, e.g.

$$\Phi(x) = \frac{SL}{2D} e^{-\frac{x}{L}}, \quad L = \sqrt{\frac{D}{\Sigma_a}} \tag{57}$$

where  $L$  is known as the diffusion length.

This theory is valid deep in the medium, where the flux  $\Phi$  is often given by multiplied scattered particles and hence it can be expected to be nearly equal in all directions, whereas near a free surface or a source the flux density is quite anisotropic and the diffusion approximation may be poor. Moreover the same hypothesis makes the theory suitable for thermal neutrons rather than fast ones [11].

The second approach becomes useful to describe a simplified behavior for fast neutrons: according to the two-group theory, neutrons in the shield are divided into neutrons at thermal energies and those above. The group diffusion Eq. 55 is applied to each group, the source term in each group being the neutrons slowed down in the immediately higher energy group. This leads to two equations of the type

$$\begin{aligned} -D_f \nabla^2 \Phi_f + \Sigma_f \Phi_f &= 0 \\ -D_t \nabla^2 \Phi_t + \Sigma_t \Phi_t - \Sigma_f \Phi_f &= 0 \end{aligned} \tag{58}$$

for the fast and the thermal group respectively. The fast source term in the shield is zero, whereas the thermal source term equals the fast neutrons scattered into thermal energies ( $\Sigma_f \Phi_f$ ) and, in a similar manner to the diffusion equation (see Eq. 57), the solution of the fast group equation in a semi-infinite plane geometry is given by

$$\Phi_f(x) = \Phi_0(x) e^{-\Sigma_R x}, \quad \Sigma_R = \frac{1}{L_s} \tag{59}$$

where  $\Sigma_R$  is the macroscopic removal cross section, which is roughly equal to the reciprocal of the average relaxation length for fast neutrons in the shielding material, and  $\Phi_0$  is the fast neutron flux at  $x = 0$ .

The theory in this case is valid until the attenuation of fast neutrons is dominated by a removal process, i.e. if concrete contains sufficient moderating material (i.e. its hydrogen content) [20].

### 2.3 The coupled thermo-hygro-mechanical problem

The NEWCON3D model consists in a series of balance equations, i.e. a mass balance equation of water (both liquid and vapour, taking into account phase changes and hydration/dehydration processes), an enthalpy balance equation of the whole multiphase medium (considering the latent heat of phase change and the hydration/dehydration process), a linear momentum balance equation of the fluid phases (Darcy’s equation) and a linear momentum balance equation of the whole medium.

Appropriate constitutive equations and some thermodynamic relationships are included as well.

The field equations of the model are briefly recalled below; for additional details the reader is referred to [1, 10, 19, 23–31, 34, 36–40].

The continuity equation for non-isothermal flow is expressed in terms of relative humidity as

$$\frac{\partial h}{\partial t} - \nabla^T \mathbf{C} \nabla h - \frac{\partial h_s}{\partial t} - k \frac{\partial T}{\partial t} + \chi \mathbf{m}^T \frac{\partial \varepsilon}{\partial t} = 0 \tag{60}$$

where  $h$  is the relative humidity,  $T$  is temperature,  $k = \left(\frac{\partial h}{\partial T}\right)_{m,\varepsilon}$  is the hygrothermic coefficient, i.e. the change in  $h$  due to one-degree change of  $T$  at constant  $m$ ,  $\varepsilon$  and a fixed degree of saturation,  $dh_s$  is the self-desiccation,  $\chi = \left(\frac{\partial h}{\partial \varepsilon_v}\right)_{T,m}$  represents the change in  $h$  due to unit change of volumetric strain  $\varepsilon_v$  at constant  $m$ ,  $T$  and a given degree of saturation,  $\mathbf{C}$  is the (relative humidity) diffusivity diagonal matrix,  $\mathbf{m}^T$  is the vector [1 1 1 0 0 0]. The last term in Eq. 60 accounts for the coupling between hygro-thermal and mechanical fields [40].

The relative humidity is expressed as the ratio between the equilibrium water vapour pressure  $p_{gw}$  and the saturation pressure  $p_{gwsat}$  through the Kelvin equation [3]

$$h = \frac{p_{gw}}{p_{gwsat}(T)} \tag{61}$$

and it is directly connected to the moisture concentration  $m$ , at variable temperature, by the sorption–desorption isotherms

$$dh = K dm + k dT + dh_s - \chi \mathbf{m}^T d\varepsilon \tag{62}$$

where  $K = \left(\frac{\partial h}{\partial m}\right)_T$  is the so-called inverse slope of desorption isotherm.

The balance equation for the relative humidity (Eq. 60) is obtained from [3], accounting for hygro-thermo-mechanical couplings, in [26, 27, 37, 38, 40].

Heat balance requires

$$\rho C_q \frac{\partial T}{\partial t} - C_a \frac{\partial m}{\partial t} - C_w \mathbf{f} \cdot \nabla T = -\Delta \mathbf{q} \tag{63}$$

where  $\rho$  is the mass density of concrete,  $C_q$  the isobaric heat capacity of concrete (per kilogram of concrete) including chemically bound water but excluding free water,  $C_a$  is the heat of sorption of free water (per kilogram of free water);  $C_w$  is the isobaric heat capacity of liquid water,  $C_w \mathbf{f} \cdot \nabla T$  is the rate of heat supply due to convection by moving water,  $\mathbf{f}$  is the flux of humidity, depending on the gradient of  $h$  by means of the permeability  $c$

$$\mathbf{f} = -c \nabla h \tag{64}$$

$\mathbf{q}$  is the heat flux which can be due to temperature gradient or moisture concentration gradient. Combining the two cases, the constitutive law defining the heat flux comes from a Fourier’s law (heat flux due to temperature gradient) and a Dufour’s flux (heat flux due to moisture concentration gradient)

$$\mathbf{q} = -a_{T_w} \nabla m - a_{T_T} \nabla T \tag{65}$$

where the coefficients  $a_{T_w}$  and  $a_{T_T}$  depend on  $m$  and  $T$ .



Finally, considering the macroscopic linear momentum balance equation for the whole medium we have

$$\text{div}\boldsymbol{\sigma} + \rho\mathbf{g} = 0 \tag{66}$$

where  $\rho$  is the density of the multiphase medium (concrete plus water species) and  $\mathbf{g}$  the acceleration related to gravity.

As regards the mechanical field, the constitutive relationship for the solid skeleton in incremental form can be written as

$$d\boldsymbol{\sigma}' = (1 - D)\mathbf{D}_T(d\boldsymbol{\varepsilon} - d\boldsymbol{\varepsilon}^T - d\boldsymbol{\varepsilon}^c - d\boldsymbol{\varepsilon}^{lits} - d\boldsymbol{\varepsilon}^p - d\boldsymbol{\varepsilon}^{sh} - d\boldsymbol{\varepsilon}^a) \tag{67}$$

where  $\boldsymbol{\sigma}'$  is the effective stress tensor according to Terzaghi ( $\boldsymbol{\sigma}' = \boldsymbol{\sigma} + p_{gw}\mathbf{I}$ ,  $\mathbf{I}$  being the identity matrix);  $D$  is the upgraded scalar radio-chemo-thermo-mechanical damage (see below),  $\mathbf{D}_T$  is the tangent stiffness matrix,  $d\boldsymbol{\varepsilon}^T$  is the strain rate caused by thermo-elastic expansion,  $d\boldsymbol{\varepsilon}^c$ , the strain rate accounting for creep,  $d\boldsymbol{\varepsilon}^{lits}$ , the load induced thermal strain rate,  $d\boldsymbol{\varepsilon}^p$ , the plastic strain rate,  $d\boldsymbol{\varepsilon}^{sh}$  is due to shrinkage and  $d\boldsymbol{\varepsilon}^a$  represents the autogenous strain increments already defined in the Sect. 2.1.1. Particularly, when only mechanical forces are taken into account,  $D$  is the damage scalar variable following the scalar isotropic model by Mazars.

According to this theory, the classical effective stress concept [19] is modified to take into account damage, measuring a reduction in the resistant area due to cracks beginning and spreading:

$$\bar{\boldsymbol{\sigma}}' = \boldsymbol{\sigma}' \frac{S}{\bar{S}} = \frac{\boldsymbol{\sigma}'}{1 - D}, \tag{68}$$

where  $S$  and  $\bar{S}$  are the resistant area of the uncracked and cracked material, respectively.

Since the damaging mechanisms are different in uniaxial tension and compression experiments, the damage parameter  $D_m$  (the subscript stands for mechanical contributions only) is decomposed into two parts,  $d_t$  for tension and  $d_c$  for compression, which are function of the equivalent strain:

$$\tilde{\varepsilon} = \sqrt{\sum_{i=1}^3 ((\varepsilon_i)_+)^2} \quad \left( (\varepsilon_i)_+ = \frac{|\varepsilon_i| + \varepsilon_i}{2} \right), \tag{69}$$

$\varepsilon_i$  being the principal strains. Hence:

$$D_m = \alpha_t d_t + \alpha_c d_c \tag{70}$$

where  $\alpha_t$  and  $\alpha_c$  are weighting coefficients defined in [29].

Thermo-chemo-mechanical damage  $D_{tc}$  has been introduced for the first time in [25]; thermo-chemical effects have been also taken into account in multiplicative way, as proposed by Gerard et al. [10] and Nechnech et al. [34] and the new  $D_{tc}$  is expected to describe thermo-chemical material degradation at elevated temperatures (mainly due to micro-cracking and cement dehydration) resulting in

reduction of the material strength properties, so that Eq. 68 becomes

$$\bar{\boldsymbol{\sigma}}' = \frac{\boldsymbol{\sigma}'}{(1 - D_m)(1 - D_{tc})} \tag{71}$$

As mentioned before, the total effect of the mechanical and thermo-chemical damages acting at the same time is multiplicative, i.e. the total damage  $D$  is defined by

$$D = 1 - (1 - D_m)(1 - D_{tc}) \tag{72}$$

The upgrade of the model has been developed by assuming that the nuclear radiation can activate a damage process which combines with the mechanical and thermo-mechanical ones so that the above multiplicative relation is maintained and the total damage is redefined

$$D = 1 - (1 - D_m)(1 - D_{tc})(1 - D_r) \tag{73}$$

in which  $D_r$  accounts for radiation damage, whose evaluation is empirically based, as reported in the following.

The application, within the numerical code NEW-CON3D, of a standard Finite Element discretization in space of Eqs. 60, 63, 66 results in

$$\begin{aligned} & \begin{bmatrix} \mathbf{K} & \mathbf{HU} & \mathbf{TU} \\ \mathbf{L}^T & \mathbf{I} & \mathbf{TP} \\ \mathbf{0} & \mathbf{TH} & \mathbf{TS} \end{bmatrix} \begin{Bmatrix} \dot{\bar{\mathbf{u}}} \\ \dot{\bar{\mathbf{h}}} \\ \dot{\bar{\mathbf{T}}} \end{Bmatrix} + \begin{bmatrix} \mathbf{0} & \mathbf{0} & \mathbf{0} \\ \mathbf{0} & \mathbf{Q} & \mathbf{0} \\ \mathbf{0} & \mathbf{0} & \mathbf{TR} \end{bmatrix} \begin{Bmatrix} \bar{\mathbf{u}} \\ \bar{\mathbf{h}} \\ \bar{\mathbf{T}} \end{Bmatrix} \\ & = \begin{Bmatrix} \dot{\mathbf{f}} + \mathbf{c} \\ \mathbf{HG} \\ \mathbf{TG} \end{Bmatrix} \end{aligned} \tag{74}$$

in which  $\bar{\mathbf{u}}, \bar{\mathbf{h}}$  and  $\bar{\mathbf{T}}$  are the nodal values of the basic variables: displacements, relative humidity and temperature,  $\mathbf{HU}$  and  $\mathbf{TU}$  account for shrinkage and thermal dilation effects, respectively;  $\mathbf{L}^T$  and  $\mathbf{TP}$  are the coupling matrices representing the influence of the mechanical and thermal field on the hygral one, respectively;  $\mathbf{Q}$  is the diffusivity matrix accounting for sorption-desorption isotherms;  $\mathbf{TH}$  the coupling matrix between the hygral and thermal fields in terms of capacity;  $\mathbf{TS}$  the matrix of heat capacity;  $\mathbf{TR}$  the matrix of thermal transmission including the convective term;  $\mathbf{c}$  the matrix accounting for creep;  $\mathbf{HG}$  the matrix of humidity variation due to drying and  $\mathbf{TG}$  accounts for heat fluxes.

For further explanations of the above terms the reader is referred to [24, 27, 40].

It has to be noticed that the constitutive relationship, given by Eq. 67 in a rate dependent formulation to account for plasticity, is consistent with the thermodynamics previously treated (see Eq. 31), if we consider that:  $d\boldsymbol{\varepsilon} - d\boldsymbol{\varepsilon}^p - d\boldsymbol{\varepsilon}^c - d\boldsymbol{\varepsilon}^T = d\boldsymbol{\varepsilon}^e$ ; the terms  $d\boldsymbol{\varepsilon}^T$  and  $d\boldsymbol{\varepsilon}^{lits}$  are responsible for the thermal effects on the strain tensor (due to low and medium-high temperatures, respectively) and, finally, the term  $d\boldsymbol{\varepsilon}^{sh}$ , responsible for shrinkage, is supposed to be due entirely to change of moisture content.

Moreover, the assumptions outlined above on the radiation field enter the model in an indirect way via the damage variable which is dependent on radiation; such a simplified approach necessarily uncouples the radiation field from the hygro-thermal ones, being instead maintained the coupling with the mechanical field through the damage variable itself. However, at this stage any other assumption could be equally questionable in the absence of more complete experimental data relating the influence of radiation diffusion within concrete on e.g. concrete moisture content and temperature, and vice versa.

### 3 Numerical analyses

The analyses have been performed to simulate the response of a concrete structure during about 50 years and by assuming a neutron flux density of  $10^{12}$  n/(cm<sup>2</sup> s), which is nearly twice the one expected for SPES and quite less than the radiation dose reached by nuclear cores (even of the order of  $10^{19}$  n/(cm<sup>2</sup> s)). The radiation flux has been supposed to be directly transmitted, unaltered, to the inner surface of the shielding, being negligible the distance between the target and the concrete wall.

Two extreme situations have been considered for neutron energies: the case in which the whole flux is given by fast neutrons and the one in which it comes totally from thermal neutrons, in order to predict the minimum and maximum threshold for radiation damage under a realistic variegated neutron spectrum, which should represent an intermediate solution.

As reported by available experimental data [15], a decay in the elastic modulus of concrete is to be expected due to nuclear radiation; such an observation has allowed for obtaining the radiation damage by interpolating the curves of decay, so evidencing the trend  $\bar{E}/E$  (elastic modulus after radiation related to the elastic modulus of the virgin material) of Fig. 1. The scattering emerging from the comparison of different test series is explained by the large variety of test conditions: concrete making materials, mix proportions of mortars, specimens size, cooling and drying conditions, impinging of fast or slow neutrons, possible simultaneous temperature exposure of specimens.

Looking at the mean behaviour, it can be observed that a neutron fluence less than  $10^{19}$  n/cm<sup>2</sup> leads to a slight decrease in the  $\bar{E}/E$  ratio, then reaching 50% under increasing neutron fluxes. Hence it has been supposed that below neutron fluxes of  $10^{18}$  n/cm<sup>2</sup> the radiation damage is zero and above  $10^{20}$  n/cm<sup>2</sup> it is constantly equal to 50%.

The available data are not sufficient to separate the effects of radiation and of heating of the samples, which in many cases they undergo in nuclear vessels conditions, however it seems reasonable to observe that the strength

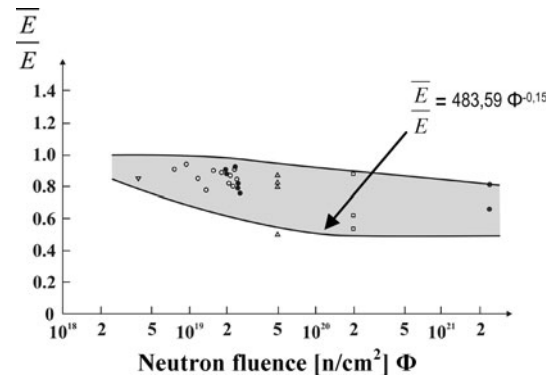


**Fig. 1** Modulus of elasticity of concrete after neutron radiation  $\bar{E}$  related to modulus of elasticity of untreated concrete  $E$  (data from [15])

loss is primarily due to neutron radiation, in analogy with similar graphs for the compressive and the tensile strength, for which a separation of the two effects was possible [15].

#### 3.1 Geometry and materials

The case study takes its origin from the SPES Project that is currently being developed at the National Laboratories of Legnaro (Padua, Italy). The facility will be directed to the production of special radioactive heavy ion beams from a primary proton beam impinging on a target made of fissionable material, where fission reactions are expected to take place, thus representing ideally a point-source of neutrons in the specific problem.

In our approach the attenuation process of neutrons in concrete is considered to be one-dimensional through the thickness of the shielding slab. This assumption is not restrictive if we consider the geometry of the problem, i.e. the diffusion of neutrons from a neutron source through a wall; the wall is modeled for a small portion qualitatively situated within the bunker building, in agreement with the design drawings provided by INFN. The neutron fluence is supposed to proceed outwards from the room through the shielding medium.

The sample analyzed is a prism 3.5 m long, with a square cross-section of 1 m<sup>2</sup>. The thickness of the model comes from radio-protection issues on the SPES facility involving the target cave that is to be kept under 0.25 mSv/h ambient dose equivalent (Spes Executive Summary 2008 [17]).

The indicated thickness relative to two different work scenarios impinging on the UC<sub>x</sub> target (radioactive ion beam of 40 MeV, 200 μA and of 70 MeV, 350 μA) are reported in Figs. 2 and 3, with the hypothetical position of the modeled portion of wall of the target cave.

The slice under analysis has been discretized by 20-nodes brick elements, with constraints on the base surface and laterally: dilations/contractions are allowed

**Fig. 2** Cross-section of the target cave with the required shielding thickness [dm] relative to two scenarios for the proton beam

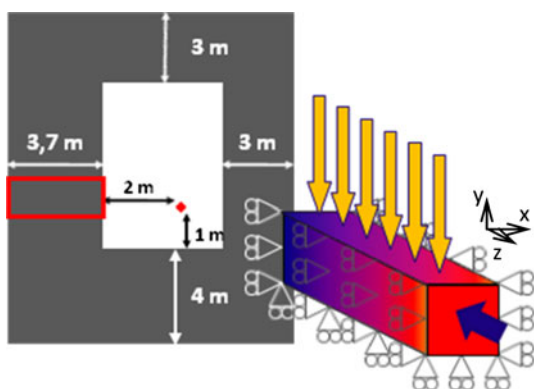
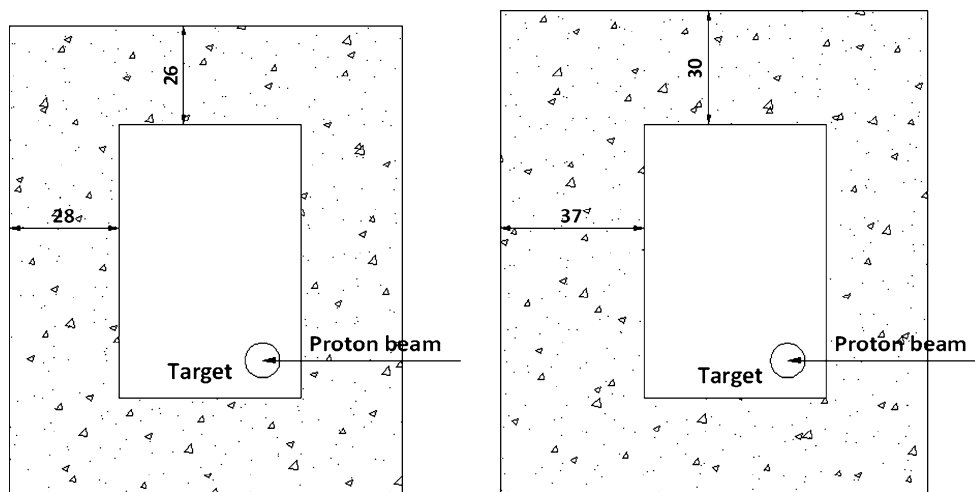


**Fig. 3** Cross-section of the target cave and investigated volume for the numerical model

along the wall thickness only; self-weight has been accounted for as well. No humidity and temperature variations have been first considered, to investigate the mechanical response due to radiation damage only. A neutron flux density of  $10^{12} \text{ n}/(\text{cm}^2 \text{ s})$  has been assumed in the calculations; the corresponding fluence (by integration of the neutron flux density in time) is supposed to proceed outwards from the room through the shielding medium, Fig. 3.

Several concrete mixtures have been compared; their application on nuclear facilities is briefly discussed below and their mechanical and shielding properties are summarized at the end of this Section, with respect to a given mixture or average values from different mixtures of the same material, the latter being the case for ordinary concrete (OPC; see Tables 1, 2).

We point out that the Young’s modulus has been derived from the empirical relation proposed by the national standard (Ministerial Decree and Circular to Ministerial Decree 2008 [5, 32]) as a function of the compressive cylinder strength, when not provided in literature:

$$E_{lcm} = 22,000 \left( \frac{f_{lcm}}{10} \right)^{0,3} \eta_E, \quad \eta_E = \left( \frac{\rho}{2,200} \right)^2, \quad (75)$$

where  $E_{lcm}$  is the average value of the secant elastic modulus after 28 days curing [Mpa],  $f_{lcm}$  is the average compressive cylinder strength [Mpa],  $\rho$  is the density of concrete [ $\text{kg}/\text{cm}^3$ ]. Concrete is supposed to behave elastically under its self-weight.

As for OPC, the average values of the main parameters are taken from eight different mixtures reported by Kaplan [20]; the assumed values are listed in Table 2.

Serpentine is a hydrous magnesium iron phyllosilicate  $[(\text{Mg}, \text{Fe})_3\text{Si}_2\text{O}_5(\text{OH})_4]$  mineral. It is used as aggregate in concrete because, as a hydrous aggregate, it can retain most of its water of crystallisation at temperatures up to about  $500^\circ\text{C}$ , thus keeping its efficiency against neutrons also in the extreme conditions of nuclear reactors. The reference values are taken from the serpentine concrete investigated by Ohgishi et al. [35].

Barites (barium sulphate– $\text{BaSO}_4$ ) is used both as coarse and as fine aggregate for concrete. The mean volumetric weight of barites concrete is about 50% higher than that of ordinary concrete and, therefore, it is more efficient than the latter against  $\gamma$ -radiation. Additionally this high specific weight aggregate has almost null reactivity with alkalis in the cement, which is understood to be one of the main causes of degradation of concrete during irradiation [16, 33]. Moreover the high neutron capture cross-section of barium ensures good shielding properties even against neutrons, though also limonite or other hydrous aggregates can be used in conjunction to improve them [21]. The assumed data for barites concrete are taken from Gallaher and Kitzes’s report [9].

Ferro-phosphorus aggregates help reaching high densities on the mortars, thus ensuring good efficiency against photons. A volume increase at temperatures above  $350^\circ\text{C}$  has been observed [20], which has been stated to be due to

**Table 1** Elemental composition of the reference mixture for serpentine (a), barites (b), limonite-steel (c), magnetite (d) concrete, in agreement with Ohgishi et al. [35], Gallaher and Kitzes [9], Davis et al. [6]

Element	(wt. %)
<i>a</i>	
MgO	33.4
SiO <sub>2</sub>	37.59
Al <sub>2</sub> O <sub>3</sub>	3.42
Fe <sub>2</sub> O <sub>3</sub>	5.15
FeO	2.04
CaO	4.82
CO	1.65
Na <sub>2</sub> O	1.13
H <sub>2</sub> O	10.26
Element	(per g/cm <sup>3</sup> of concrete)
<i>b</i>	
H in water	0.0243
O in water	0.195
in Ore	0.872
in cement	0.118
Mg in water	0.00385
Al in water	0.0137
Si in water	0.0352
S	0.364
Ca in ore	0.0203
in cement	0.147
Fe in ore	0.151
in cement	0.0091
Ba	1.551
Element	(per g/cm <sup>3</sup> of concrete)
<i>c</i>	
H	0.028
O	0.806
Mg	0.039
Al	0.078
Si	0.078
Ca	0.25
Ti	–
Mn	–
Fe	3.03
Element	(wt. %)
<i>d</i>	
Fe	55.9
O	34.4
Ca	6.6
Si	1.6
H	0.7
Al	0.6
Mg	0.2

**Table 2** Assumed values for mechanical and shielding properties of the analyzed concretes, in agreement with Kaplan [20], Ohgishi et al. [35], Gallaher and Kitzes [9], Davis et al. [6]

Type of concrete	Density $\rho$ (kg/m <sup>3</sup> )	$f_{ck}$ (MPa)	$E$ (MPa)	$\Sigma_R$ (cm <sup>-1</sup> )	L (cm)
Ordinary	2.33	25	32.484	0.0787	8.0434
Serpentine	2.09	19.3	24.069	0.0836	2.11
Barytes	3.5	24.8	31.157	0.0819	5.4928
Ferro-phosphorus	4.65	30.4	28.200	0.119	2.2045
Limonite-steel	4.27	38.4	47.900	0.1158	2.1016
Magnetite	3.41	41.8	57.800	0.1061	3.0367

accelerated rates of oxidation of the aggregate. It has also been reported that ferro-phosphorus concretes may lead to the production of inflammable gases that could develop high pressures if confined and that they experience delay in setting and hardening. The quantities of interest, herein, refer to ferro-phosphorus concretes used for the N-Production Reactor at Hanford in the USA [6]; no chemical composition has been found for it.

Limonite (FeO(OH)·nH<sub>2</sub>O) ores are hydrous iron ores used in concrete primarily because of their high content of chemically combined water (twice as high a concentration of water as an ordinary concrete may be achieved), thus improving the effectiveness of shielding against neutron flux. Limonite retains its water of crystallisation up to 200°C. Fine limonite aggregate which gives sufficient plasticity to the concrete mix for casting is used for heavy concretes with the addition of metal scrap (steel punching, sheared bars, steel shots). The collected data are of a limonite-steel from Hanford [6].

Magnetite (Fe<sub>3</sub>O<sub>4</sub>) is used as heavy aggregate for special concrete. Its water content is not as high as in limonite and, consequently, it has lower shielding properties. The reference mortar is taken again from [6].

In Tables 1 and 2 the available chemical composition of the investigated improved concrete mixtures and their mechanical and nuclear properties have been reported, respectively, whereas Table 3 lists additional hygro-thermo-mechanical parameters for the development of the numerical analyses. Particularly, the damage law is the one by Mazars [28, 29], creep is accounted for referring to the Maxwell chain model for the relaxation function  $R(t, t')$  of Eq. 45, in the form of the double power law by Bazant and Osman [4].

### 3.2 Numerical results and validation

The results have been collected mainly in terms of damage parameter versus distance. Due to the negligible effect of compression from self-weight load, damage can be

**Table 3** Material data for numerical analyses

Poisson's ratio	0.2
Permeability/g (isotropic)	40 mm <sup>2</sup> /days
Thermal expansion coefficient	10 <sup>-6</sup> °C <sup>-1</sup>
Specific heat	880 J/(kg °C)
Heat conductivity (isotropic)	0.13 × 10 <sup>-2</sup> J/(mm °C s)
Hygrothermic coefficient <i>k</i>	0.005°C <sup>-1</sup>
Coefficient $\chi$ for $h = 0$	0.004
Damage parameters according to Mazars' model (1984–1989)	
Triggering of damage ( $K_0$ )	0.1 × 10 <sup>-3</sup>
$A_r$	1
$B_r$	2,000
$A_c$	1.4
$B_c$	1545
Maxwell chain model	
Number of Maxwell units	8
Double creep law parameters Bazant and Osman [4] (time in days)	
$E_0$	70,836 MPa
$\varphi_1$	4.5
$m$	0.296
$\alpha$	0.076
$n$	0.181

considered as totally due to radiation. The results (referring to the material data of Table 3) are reported in Fig. 4 in terms of displacements  $u_y$ , principal stress  $\sigma_y$  (with  $y$  loading direction) and total damage  $D$  as functions of the irradiation time on OPC; the results refer to a node belonging to the directly impinging concrete surface. The radiation field is characterized by a neutron flux density of  $10^{12}$  n/(cm<sup>2</sup> s), integrated on 50 years duration span.

Damage reaches its maximum (50%) after 5–10 years and correspondingly stresses reach their equilibrium value; differently, a delay in the occurrence of the asymptotic (steady) value for displacements is shown, accompanied by the occurrence of a moderate expansion after the peak value: such a behaviour is referable to concrete creep. The stress state is strongly affected by radiation, generating the inability of concrete for sustaining even low compression values at the expense of larger deformations. Longer radiation exposure leads to more pronounced trends.

In agreement with the empirical curves of Fig. 1, the obtained stress–strain curve is shown in Fig. 5, where 50% decay in the elastic modulus of concrete is evidenced (as expected) due to radiation damage.

In agreement with the diffusion theory for thermal neutrons and the two-group theory for fast neutrons, the damage behavior as function of depth for OPC has been investigated. Figure 6 shows the influence of thermal and fast neutrons on the development of damage versus distance from the exposed surface: when fast neutrons are

impinging, the damaged thickness is more pronounced and, specifically, the amount of the damaged thickness induced by fast neutrons exceeds the one induced by thermal neutrons of 80% of the latter, at 5 years radiation and of 70% of it, at 50 years radiation.

Special concretes (i.e. improved mixtures) have been additionally accounted for in the following, for a fast and a thermal neutron flux of  $10^{12}$  n/(cm<sup>2</sup> s) integrated in 1 year exposure, respectively (Fig. 7): all the mixtures show better shielding properties than OPC, particularly magnetite, limonite-steel and ferro-phosphorus for fast neutrons and serpentine, limonite-steel and ferro-phosphorus for thermal neutrons.

For validation purposes, the results have been additionally compared with the experimental evidences provided by Elleuch et al. [7] who have studied the behavior under irradiation of special shielding concretes; specifically, changes in properties of a serpentine concrete irradiated at fast-neutron fluences of  $3 \times 10^{19}$  and  $10^{20}$  n/cm<sup>2</sup> have been accounted for. The values of the elastic moduli at different radiation exposures have been estimated indirectly, by measuring the propagation times of an ultra-sonic wave longitudinally transmitted on each sample, in order to avoid the definition of the Poisson's coefficient for the irradiated samples.

The authors have found decays in the Young's moduli of about 40% and 45%, for the two fluences respectively, if compared to that of not irradiated control specimens, cured at 20°C and 60% relative humidity.

The test has been numerically reproduced by taking into account a sample made with serpentine concrete, assigning the same neutron fluences at one face, supposing an exponential decay within the thickness, according to Eq. 59. The decay in the elastic modulus related to the not irradiated condition is reported in Fig. 8, referring to a point close to the directly exposed face. The predicted results are in agreement with the experimental test, confirming that the upgrade of NEWCON3D is able to describe the ultimate strength of concrete, when affected by radiation.

Additional simulations have been then performed in conjunction with a Monte Carlo code developed by CERN and INFN of Milan, Fluka [8], used to describe the radiation field (neutron fluence and deposited energy) which the mechanical field is dependent on. The objective has been now to take into account the collateral effect represented by the development of heat within the shielding, consequent to absorbed radiation, as long as the power density is not negligible, i.e. for values of energy flux density above  $10^{10}$  MeV/(cm<sup>2</sup> s); correspondingly, the coupled hygro-thermal response of concrete has been now evaluated.

The same geometry as of Fig. 3 has been implemented in Fluka, in order to obtain an estimate of the main physical



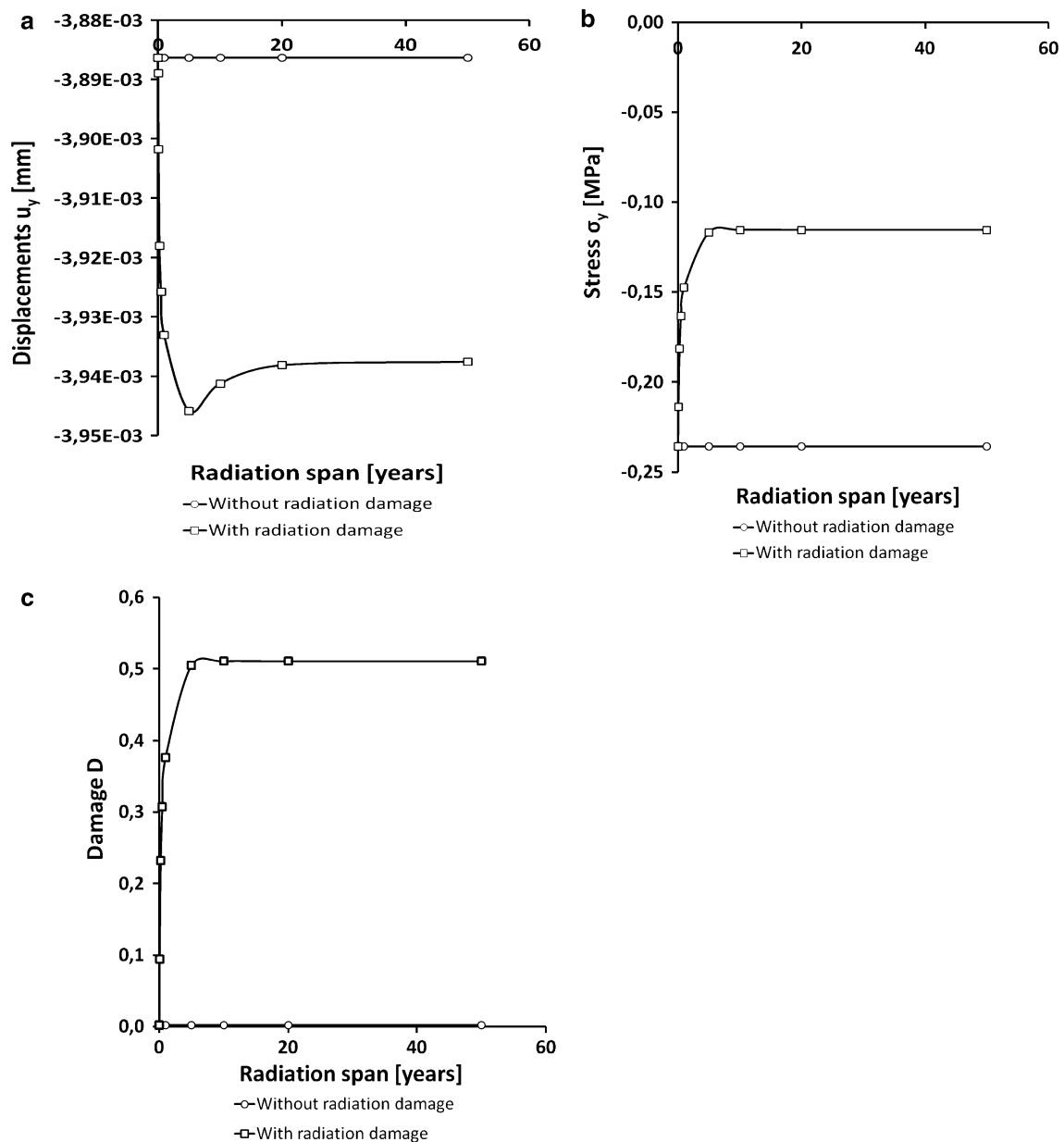


**Fig. 4** Displacements  $u_y$  (a), principal stress  $\sigma_y$  (b) and total damage  $D$  (c) as functions of the radiation span on OPC, close to the directly exposed surface, both in case that radiation damage is or not activated

quantities affecting the problem: neutron fluence and energy deposition. The former, which the decay in the Young modulus is function of, is directly responsible for the quantification of the radiation damage; the latter allows for determining the boundary conditions in terms of temperature, at the wall exposed surface.

The geometry in Fluka is assigned by means of elemental volumes (planes, spheres, parallelepipeds, regular prisms...) and Boolean operations between them (addition, subtraction, union) applied to describe “regions” made of different materials. Each portion of space needs to be assigned to one region only.

As regards concrete, the chemical composition of an ordinary concrete in percentage by weight provided in [20] has been adopted (Table 4).

The target of fissionable material has the dimension of seven disks (uranium and carbon compounds) for a total mass of 30 g, a radius of 2 cm and thickness of about 1.3 mm, which makes it an ideal point-source of neutrons.

The impinging beam starts at an arbitrary point inside a vacuum pipe; thanks to the vacuum environment, it is therefore supposed to be delivered not attenuated to the target. The characteristics of the primary proton beam

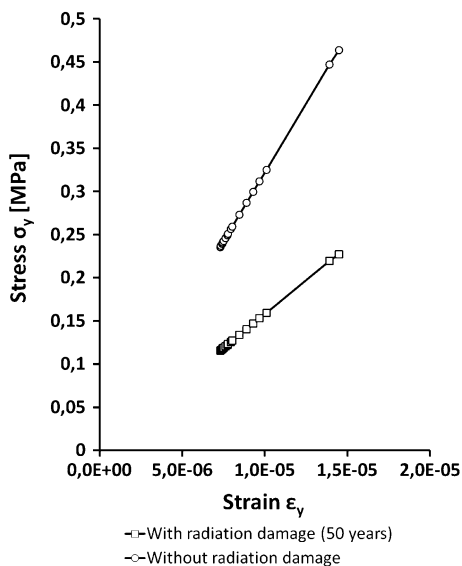


**Fig. 5** Stress-strain relation along direction  $y$ , loading direction, for OPC, near the most exposed surface, after a 50 years long radiation span

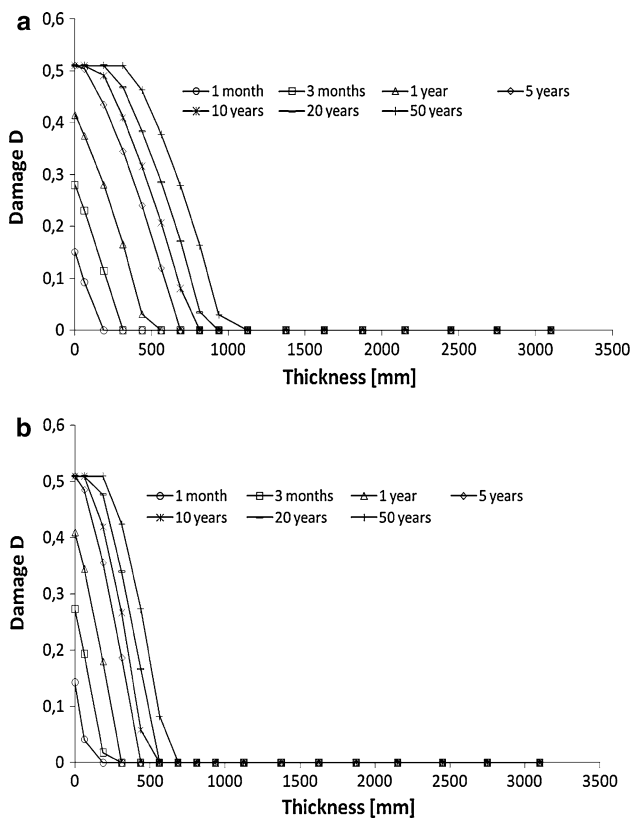


**Fig. 6** Radiation damage progression with depth of the sample under radiation fluence up to 50 years, from fast neutrons (a) and thermal neutrons (b) on OPC

come from the most serious exercise scenario designed by INFN for the SPES facility, as reported before. The stochastic simulation with Fluka required 3 cycles per run,

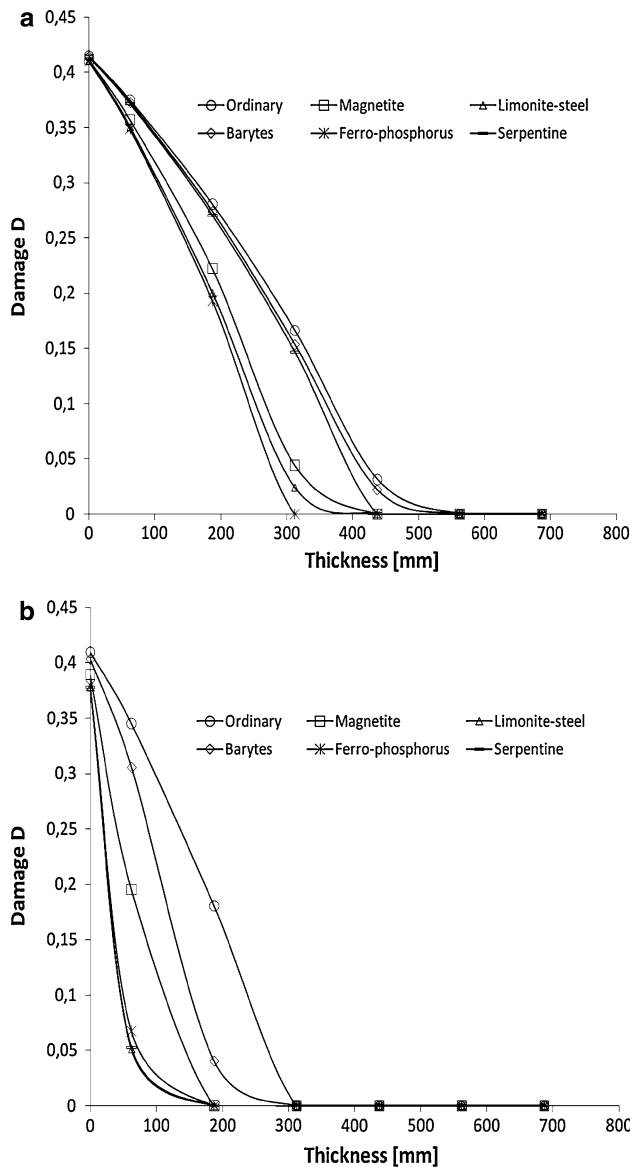


**Fig. 7** Radiation damage progression with depth of the sample under the radiation fluence of 1 year, from fast neutrons (a) and thermal neutrons (b) on ordinary and special shielding concretes

with  $10^6$  primary particles launched at each run, in order to reach acceptable statistics.

Fluka results are provided on a regular parallelepiped grid, at the centre of mass for each element, the dimensions of which are determined by the required results resolution. A regular grid of small elements 5 cm wide along each direction has been adopted for our study. A subsequent interface program has been additionally used to pass results from the centre of mass for each volume of the results' grid to the FEM mesh adopted in NEWCON3D, based on the algorithm of the minimum distance.

In Fig. 9 the map of neutron flux density for the control volume corresponding to the mesh analyzed in

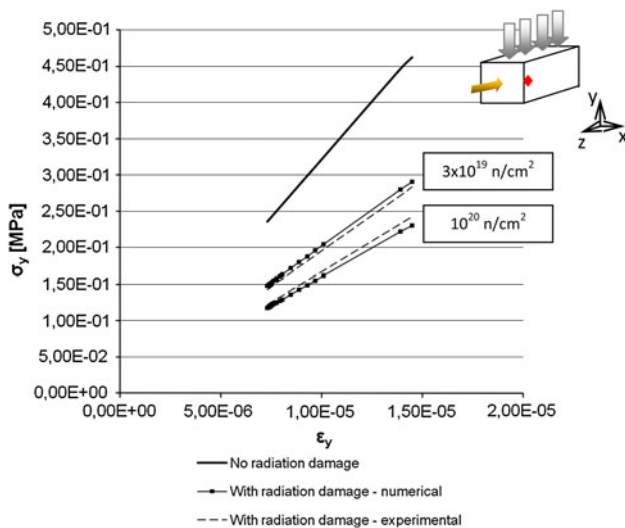
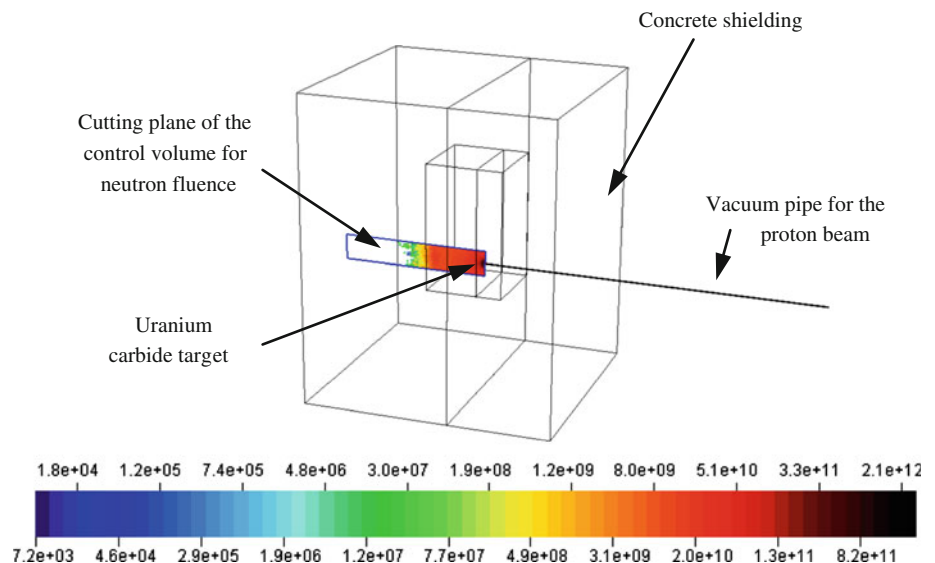


**Fig. 8** Validation of the numerical model with experimental results by Elleuch et al. [7]

**Table 4** Assumed chemical composition for the ordinary concrete implemented in Fluka [20]

Element	% by weight (%)	Element	% by weight (%)
Hydrogen	0.64	Phosphorus	0.09
Oxygen	45.36	Sulphur	0.09
Carbon	–	Potassium	0.64
Sodium	1.76	Calcium	12.66
Magnesium	3.66	Titanium	0.47
Aluminium	5.88	Iron	0.13
Silicon	20.90	Nickel	7.64
Concrete density [g/cm <sup>3</sup> ]	2.33		

**Fig. 9** Neutron flux density for the control volume corresponding to the FEM mesh implemented in NEWCON3D. Results from Fluka on the cutting plane just in front of the source [n/(cm<sup>2</sup>s)]



NEWCON3D is evidenced, which is of interest being expected to be the most exposed; the first meter of wall only seems to be affected by neutron absorption, and these values have been transferred to the corresponding volume in NEWCON3D.

In Fig. 10 the results in terms of deposited energy are shown, for a wider investigated area of the shielding. Results refer to prompt radiation, i.e. the instantaneous component of the total amount of deposited energy; they are here intended for primary incident particle (i.e. per proton) and need to be normalized in order to reach total values of power density.

For a better visualization, Fig. 11 depicts the same values of neutron flux and power density (here normalized), for the same directly exposed investigated prism and the same geometric cutting planes. The order of magnitude of the maximum neutron flux density is proved to be 10<sup>10</sup> n/(cm<sup>2</sup> s); the maximum power density is 10<sup>10</sup> GeV/(cm<sup>3</sup> s).

Neutron flux density, integrated in time of exposure to radiation (thus getting neutron fluence), is intended to enter NEWCON3D as the parameter directly affecting radiation damage; power density has been used to estimate the temperature field in concrete due to heat production by radiation, particularly to impose boundary conditions for temperature at the outer face of the prism modeled in NEWCON3D.

The temperature rise has been quantified via a transient thermal analysis and then applied as a time variable boundary condition to the F.E. model. In Fig. 12 the contour map of temperature for a neutron source working continuously for 6 months is shown.

Figure 12 evidences that the maximum temperature is encountered at the corner close to the source, where after 6 months nearly 70°C are reached; in the last picture a time

**Fig. 10** Energy deposition on the directly exposed area of the concrete shielding. Results from Fluka on the cutting plane just in front of the source [GeV/(cm<sup>3</sup> primary)]

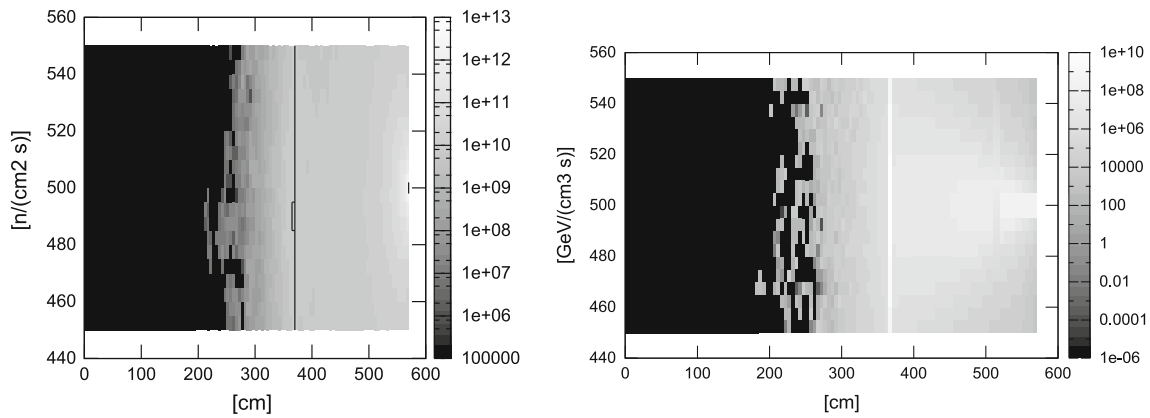
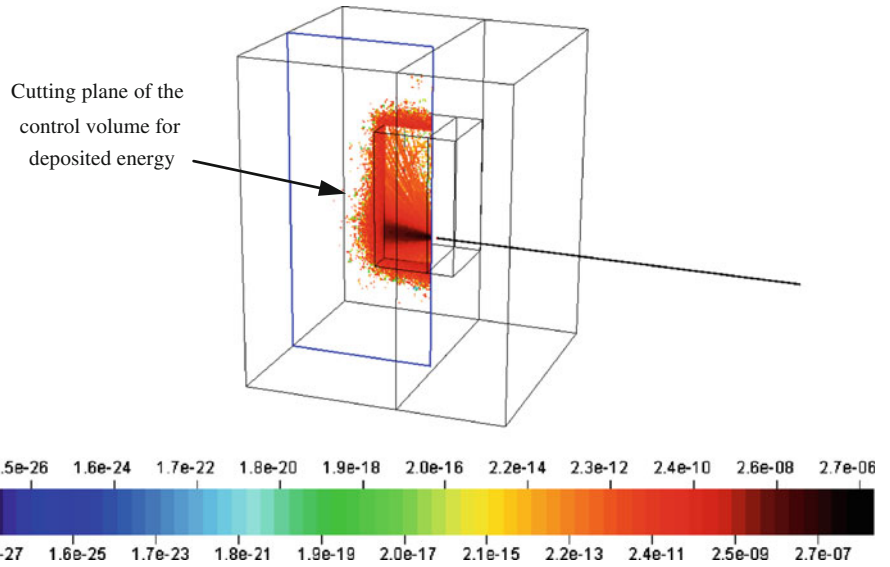


**Fig. 11** Neutron flux density [n/(cm<sup>2</sup> s)] and power density [GeV/(cm<sup>3</sup> s)] on the cutting plane of the directly exposed control volume

**Fig. 12** Temperatures on the directly impinged zone after 6 months of work for the facility

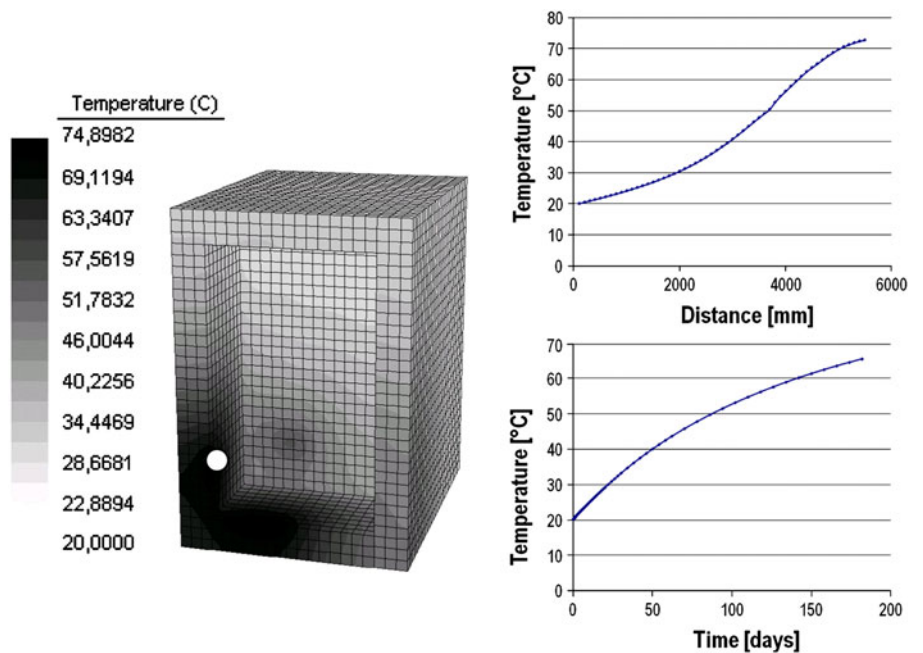


**Fig. 13** Contour maps of relative humidity after 1 h, 1 week, 6 months [–]

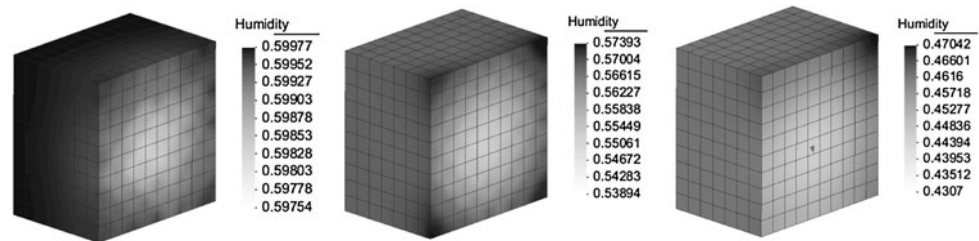
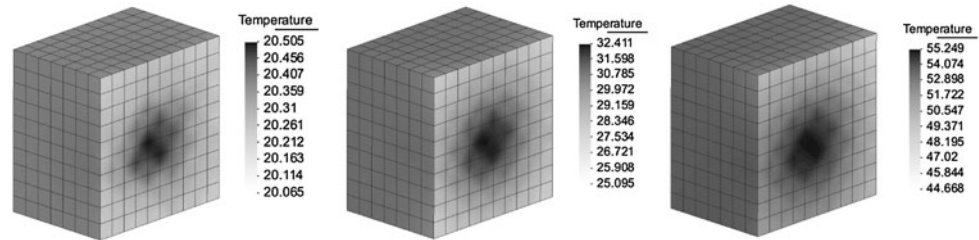


**Fig. 14** Contour maps of temperature after 1 h, 1 week, 6 months [°C]



history for the same critical node is reported, which shows a parabolic increase in time.

The effect is shown to be not negligible, which is in agreement with the requirements of ANSI/ANS-6.4-1985, according to which radiation heat and subsequent thermal effects are to be taken into account for energy flux densities (power densities) above  $10^{10}$  MeV/(cm<sup>2</sup> s).

It is to be noticed that Fig. 11 gives maximum values of the order of magnitude of  $10^{10}$  GeV/(cm<sup>3</sup> s), where cm<sup>3</sup> are to be intended per volume of the small elements defined by the resolution of the result grid (side of the cubes: 5 cm), therefore one gets  $5 \times 10^{10}$  GeV/(cm<sup>2</sup> s), which is quite above the prescribed limit required to neglect thermal effects. In fact, thermal effects are now understood to be mainly responsible for the stress state of the shielding, as it will be better illustrated in the results obtained from the thermo-hygro-mechanical analysis.

The thermal analysis justifies also the working period of the facility assumed in the study, i.e. 6 months, nearly 4,500 h per year, longer durations resulting unacceptable for the material.

Back-analyses with Fluka have been made in order to study the influence of radiation heat in the variation of water content of concrete, but no significant change in the neutron fluence has been envisaged; this has allowed for concluding that the experimented deposited energies do not provide significant losses in the shielding properties of concrete; i.e. the slight variations in water content, due to radiation heat, have not shown to affect the moderating capacity of concrete towards neutrons, namely due to the intrinsic hydrogen content given by its bound water.

Initial conditions consider an internal relative humidity of 60% and a temperature of 20°C; the results from the hydro-thermo-mechanical analysis are reported in Figs. 13, 14, 15 (only a portion of the model is here shown); particularly, Fig. 15 depicts damage, longitudinal displacements, relative humidity and temperature, respectively, along the prism central axis and a parallel line at its border.

Relative humidity seems to be not much affected by the 6 months prolonged radiation, whereas temperature rise is understood to be of interest, leading to thermal gradients up to 50°C; for this reason the irradiation profile for the SPES facility should not exceed 4,500–5,000 h/year, i.e. nearly 6–7 months of continuous service, within the investigated exercise scenario (once specifics on the primary proton beam and geometry of the target cave are assigned).

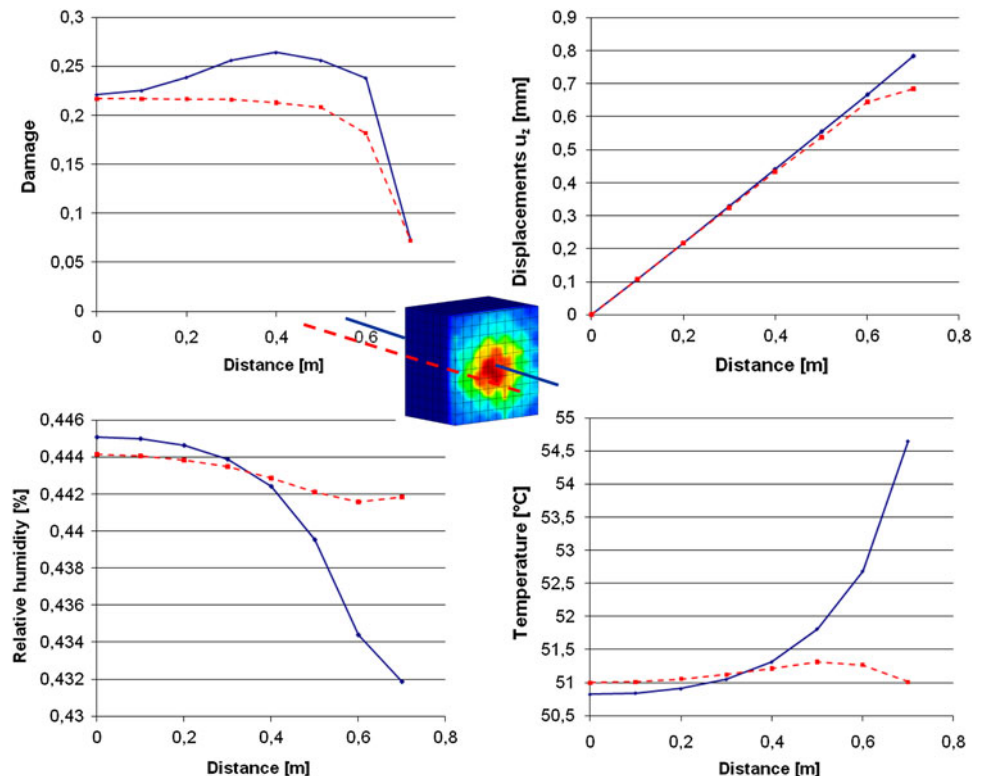
As regards the results in terms of damage, this is intended to be due only to thermo-chemical effects, since now the neutron fluence, for the investigated time span, stays always under the critical value of  $10^{19}$  n/cm<sup>2</sup>, which is expected to mark the beginning of first evidences of damage by radiation in concrete; therefore, now, the thermal aspect of the problem represents the most restrictive condition to prescribe the period of work for the facility as well as to define its structural integrity.

## 4 Conclusions

Nuclear radiation both in the form of fast and thermal neutrons is known to affect concrete in its mechanical behavior over peculiar threshold quantities of radiation



**Fig. 15** Distribution of the main variables after 6 months along the first 0.7 m wall thickness (reference lines: prism central axis and parallel axis at the border)



fluence. To our purposes, radiation in the form of neutron particles has been of particular interest, since the estimate of durability performances of the shielding walls for SPES target room, where the fissionable target represents the neutron source, is the expected utility of this study.

A collection of the most relevant experimental results on neutron irradiated concrete has been exploited to derive a formulation for radiation damage in the context of damage mechanics for concrete materials. An upgraded parameter has been introduced in a F.E. research code assessing the coupled hygro-thermo-mechanical behavior of concrete. Total damage is the result of a multiplicative relationship, accounting for radiation, as well as thermo-chemo-mechanical damage, the latter being already implemented in the constitutive law of the material, so that the two effects are independent on each other, when not present simultaneously.

Results in terms of damage have been achieved, also taking into account several kinds of special concrete commonly used for reactor shielding, which allows for defining up to a 50 years long radiation exposure the edge of the damaged portion of wall, when a neutron flux density of  $10^{12}$  n/(cm<sup>2</sup> s) is supposed to impinge the biological shielding under the assumptions of the approximated diffusion theory and two-group theory for thermal and fast neutron fluences, respectively.

The numerical code in its upgraded form, taking into account the effect of radiation damage, is thus expected to

describe the mechanical response of concrete when irradiated; in particular, under the considered irradiation scenario, OPC has shown a decrease in its elastic modulus of nearly 50%, thus providing a low strength capacity to external loads; when considering improved mixtures, under equal fluences, strength is less affected by damage so that special concretes are preferable not only for shielding requirements but also from a purely mechanical point of view.

As an alternative approach, Monte Carlo stochastic techniques have been considered to catch the complexity of the interaction of radiation with concrete, also in terms of collateral reactions to its attenuation on the shielding material.

The coupling between radiation and hygro-thermal fields to check the joint effects of prolonged irradiation exposures on concrete behaviour has been additionally focused.

## References

1. Baggio P, Majorana CE, Schrefler BA (1995) Thermo-hygro-mechanical analysis of concrete. *Int J Num Meth Fluids* 20:573–595
2. Bazant ZP, Huet C (1999) Thermodynamic functions for ageing viscoelasticity: integral form without internal variables. *Int J Solids Struct* 36:3993–4016

3. Bazant ZP, Najjar LJ (1972) Nonlinear water diffusion in non-saturated concrete. *Matériaux et constructions* 25(5):3–20
4. Bazant ZP, Osman E (1976) Double power law for basic creep of concrete. *Matériaux et constructions (RILEM, Paris)* 49(9):3–11
5. Circular 02-02-2009, n. 617 (2009) Instructions for the application of the “New technical standard for constructions”: Ministerial Decree 14-01-2008 (in Italian)
6. Davis HS, Browne FL, Witter HC (1956) Properties of high-density concrete made with iron aggregate. *J Amer Concr Inst* 52(3):705–726
7. Elleuch MF, Dubois F, Rappeneau J (1972) Effects of neutron radiation on special concretes and their components. *Amer Concr Inst Special Publication SP-34: Concrete for nuclear reactors*, Paper SP34-51:1071–1108
8. Fassò A, Ferrari A, Ranft J, Sala PR (2005) FLUKA: a multi-particle transport code. CERN-2005-10, INFN/TC\_05/11, SLAC-R-773
9. Gallaher RB, Kitzes AS (1953) Summary report on Portland cement concretes for shielding. USAEC report ORNL-1414
10. Gerard B, Pijaudier-Cabot G, Laborde C (1998) Coupled diffusion-damage modeling and the implications on failure due to strain localization. *Int J Solids Struct* 35(31–32):4107–4120
11. Harrison JR (1958) Nuclear reactor shielding. Temple Press, London
12. Hayakawa K, Murakami S, Liu Y (1998) An irreversible thermodynamics theory for elastic-plastic-damage materials. *Eur J Mech, A/Solids* 17(1):13–32
13. Hazanov S (1995) New class of creep-relaxation functions. *Int J Solids Struct* 32(2):165–172
14. Hazanov S (1997) On separation of energies in viscoelasticity. *Mech Res Commun* 24(2):167–177
15. Hilsdorf HK, Kropp J, Koch HJ (1978) The effects of nuclear radiation on the mechanical properties of concrete. In: Douglas McHenry international symposium on concrete and concrete structures. *Amer Concr Inst Special Publication SP 55-10*, Detroit, Michigan, pp 223–251
16. Ichikawa T, Koizumi H (2002) Possibility of radiation-induced degradation of concrete by alkali-silica reaction of aggregates. *J Nucl Sci Technol* 39(8):880–884
17. INFN-LNL-224 (2008) SPES selective production of exotic species: executive summary. In: Covello A, Prete G (eds) National Laboratories of Legnaro, Legnaro, Padua
18. Ireman P, Klarbring A, Stromberg N (2003) A model of damage coupled to wear. *Int J Solids Struct* 40:2957–2974
19. Kachanov MD (1958) Time of rupture process under creep conditions. *Izvestia Akademii Nauk* 8:26–31 (in Russian)
20. Kaplan MF (1989) Concrete radiation shielding: nuclear physics, concrete properties, design and construction. Wiley, New York
21. Komarovskii AN (1961) Shielding materials for nuclear reactors. Pergamon Press, London
22. Lemaitre J, Chaboche J-L (1988) Mechanics of solid materials. Dunod, Paris (in French)
23. Lewis RW, Schrefler BA (1987) The finite element method in the deformation and consolidation of porous media. Wiley, New York, (Chapter 9 with C. Majorana, Two-dimensional, non-linear, thermo-elasto-plastic consolidation program PLASCON, pp 207–333)
24. Majorana CE, Salomoni VA (2004) Parametric analyses of diffusion of activated sources in disposal forms. *J Hazard Mat* A113:45–56
25. Majorana CE, Saetta A, Scotta R, Vitaliani R (1995) Mechanical and durability models for lifespan analysis of bridges. IABSE Sym.: extending the lifespan of structures, San Francisco, CA, USA 23–25:1253–1258
26. Majorana CE, Salomoni VA, Secchi S (1997) Effects of mass growing on mechanical and hygrothermic response of three-dimensional bodies. *J Mat Process Technol* PRO064/1–3:277–286
27. Majorana CE, Salomoni VA, Schrefler BA (1998) Hygrothermal and mechanical model of concrete at high temperature. *Mat Struct* 31:378–386
28. Mazars J (1984) Application de la mécanique de l’endommagement au comportement non linéaire et la rupture du béton de structure. Ph.D. dissertation, L.M.T., Université de Paris, France
29. Mazars J (1989) Description of the behaviour of composite concretes under complex loadings through continuum damage mechanics. In: Lamb JP (ed) Proceedings of 10th US national congress of applied Mech, ASME
30. Mazars J, Pijaudier-Cabot G (1989) Continuum damage theory: application to concrete. *J Engrg Mech ASCE* 115:345–365
31. Mazars J, Pijaudier-Cabot G (1996) From damage to fracture mechanics and conversely: a combined approach. *Int J Solids Struct* 33:3327–3342
32. Ministerial Decree 14-01-2008 (2008) “New technical standard for constructions” (in Italian)
33. Naus DJ (2007) Primer on durability of nuclear power plant reinforced concrete structures: a review of pertinent factors. Oak Ridge National Laboratory, U.S. Nuclear Regulatory Commission Office of Nuclear Regulatory Research Washington, DC
34. Nechnech W, Reynouard JM, Meftah F (2001) On modeling of thermo-mechanical concrete for the finite element analysis of structures submitted to elevated temperatures. In: De Borst R, Mazars J, Pijaudier-Cabot G, van Mier J (eds) Proceedings of fracture mech of concrete structures, pp 271–278
35. Ohgishi S, Miyasaka S, Chida J (1972) On properties of magnetite and serpentine concrete at elevated temperatures for nuclear reactor shielding. *Amer Concr Inst Special Publication SP-34: concrete for nuclear reactors*, paper SP34-57:1243–53
36. Salomoni VA, Majorana CE, Khoury GA (2007a) Stress-strain experimental-based modeling of concrete under high temperature conditions. In: Topping BHV (ed) Civil engineering computations: tools and techniques, Ch 14. Saxe-Coburg Publications, pp 319–346
37. Salomoni VA, Mazzucco G, Majorana CE (2007) Mechanical and durability behavior of growing concrete structures. *Eng Comput* 24(5):536–561
38. Salomoni VA, Majorana CE, Giannuzzi GM, Miliozzi A (2008) Thermal-fluid flow within innovative heat storage concrete systems for solar power plants. *Int J Num Meth Heat Fluid Flow (Special Issue)* 18(7/8):969–999
39. Salomoni VA, Majorana CE, Mazzucco G, Xotta G, Khoury GA (2009) Multiscale modelling of concrete as a fully coupled porous medium. In: Sentowski JT (ed) Concrete Materials: properties, performance and applications, Ch 3. Nova Science Publishers Inc, New York
40. Schrefler BA, Simoni L, Majorana CE (1989) A general model for the mechanics of saturated-unsaturated porous materials. *Mat Str* 22:323–334
41. Shultis JK, Faw RE (1996) Radiation shielding. Prentice Hall PTR, Englewood Cliffs
42. Staverman AJ (1954) Thermodynamics of linear viscoelastic behavior. In: Proceedings of second international congress on rheology. Academic Press, New York, pp 134–138
43. Staverman AJ, Schwarzl F (1952) Thermodynamics of viscoelastic behaviour. In: Proceedings of Acad Sci Amst. The Netherlands, B55, pp 474–490
44. Weitsman Y (1990) A continuum diffusion model for viscoelastic materials. *J Phys Chem* 94:961–968